

Supplementary Material

Monarubins A–C from the Marine Shellfish-Associated Fungus *Monascus ruber* BB5

Yan-Qin Ran ¹, Wen-Jian Lan ², Yi Qiu ³, Qi Guo ³, Gong-Kan Feng ⁴, Rong Deng ⁴, Xiao-Feng Zhu ⁴, Hou-Jin Li ^{3,*}, and Jun Dong ^{1,*}

¹ School of Traditional Chinese Medicine, Guangdong Pharmaceutical University, Guangzhou 510006, China; ranyq03@163.com (Y.-Q.R.)

² School of Pharmaceutical Sciences, Sun Yat-sen University, Guangzhou 510006, China; lanwj@mail.sysu.edu.cn (W.-J.L.)

³ School of Chemistry, Sun Yat-sen University, Guangzhou 510275, China; qiuyi0771@163.com (Y.Q.); guoqi1228@126.com (Q.G)

⁴ State Key Laboratory of Oncology in South China, Collaborative Innovation Center for Cancer Medicine, Cancer Center, Sun Yat-sen University, Guangzhou 510060, China; fenggk@sysucc.org.cn (G.-K.F.); dengrong@sysucc.org.cn (R.D.); zhuxfeng@mail.sysu.edu.cn (X.-F.Z.)

* Correspondence: ceslhj@mail.sysu.edu.cn (H.-J.L.); Dongjun@gdpu.edu.cn (J.D.); Tel: +86-20-84113698 (H.-J.L.); 86-13822726106 (J.D.)

List of contents:

Figure S1. HR-(+) ESI-MS spectrum of monarubin A (1).	6
Figure S2. ¹ H NMR spectrum of monarubin A (1) in CDCl ₃ (500 MHz).	7
Figure S3. ¹³ C NMR spectrum of monarubin A (1) in CDCl ₃ (125 MHz).....	8
Figure S4. DPET 135 spectrum of monarubin A (1) in CDCl ₃ (125 MHz).....	9
Figure S5. HMQC spectrum of monarubin A (1) in CDCl ₃	10
Figure S6. ¹ H– ¹ HCOSY spectrum of monarubin A (1) in CDCl ₃	11
Figure S7. HMBC spectrum of monarubin A (1) in CDCl ₃	12
Figure S8. NOEY spectrum of monarubin A (1) in CDCl ₃	13

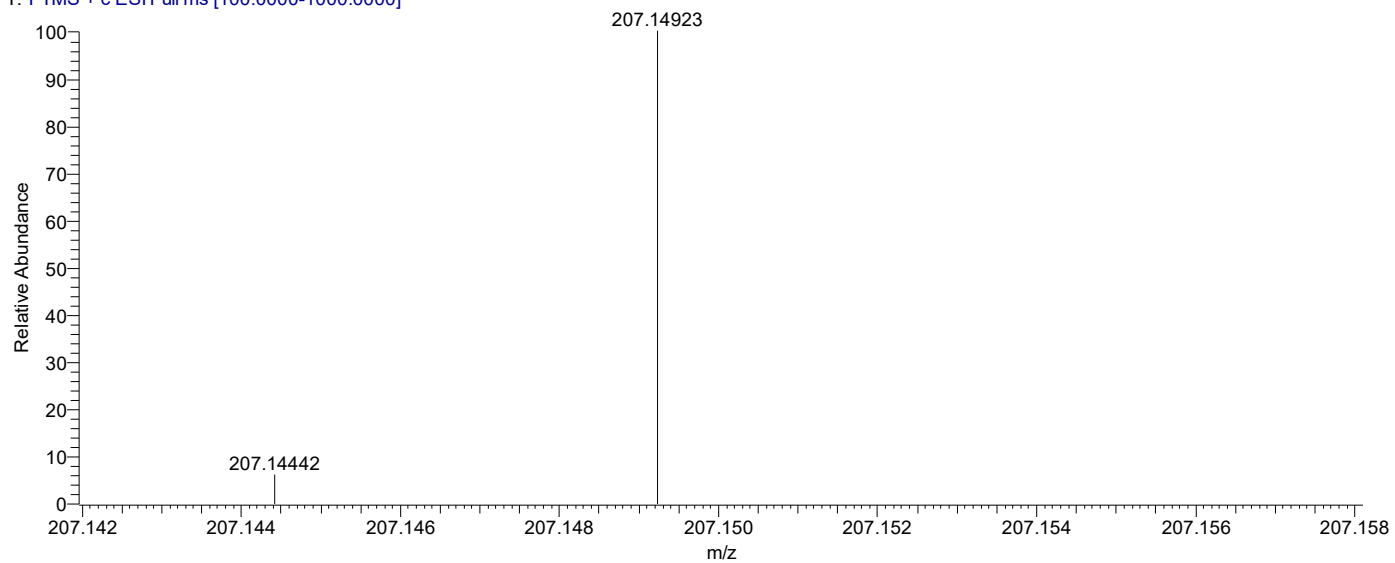
Figure S9. ¹ H NMR spectrum of 3,6-diisobutyl-2(1 <i>H</i>)-pyrazinone (2) in CDCl ₃ (400 MHz).	14
Figure S10. ¹³ C NMR spectrum of 3,6-diisobutyl-2(1 <i>H</i>)-pyrazinone (2) in CDCl ₃ (100 MHz).	15
Figure S11. HR-(+) ESI-MS spectrum of deoxyhydroxyaspergillic acid (3).	16
Figure S12. ¹ H NMR spectrum of deoxyhydroxyaspergillic acid (3) in CDCl ₃ (400 MHz).	17
Figure S13. ¹³ C NMR spectrum of deoxyhydroxyaspergillic acid (3) in CDCl ₃ (100 MHz).	18
Figure S14. HR-(+) ESI-MS spectrum of 2-hydroxy-6-(1-hydroxy-1-methylpropyl) 3- <i>sec</i> -butylpyrazine (4).	19
Figure S15. ¹ H NMR spectrum of 2-hydroxy-6-(1-hydroxy-1-methylpropyl) 3- <i>sec</i> -butylpyrazine (4) in CDCl ₃ (400 MHz).	20
Figure S16. ¹³ C NMR spectrum of 2-hydroxy-6-(1-hydroxy-1-methylpropyl) 3- <i>sec</i> -butylpyrazine (4) in CDCl ₃ (100 MHz).	21
Figure S17. ¹ H NMR spectrum of pulchellalactam (5) in CDCl ₃ (400 MHz).	22
Figure S18. ¹³ C NMR spectrum of pulchellalactam (5) in CDCl ₃ (100 MHz).	23
Figure S19. HR-(+) ESI-MS spectrum of monarubin B (6).	24
Figure S20. ¹ H NMR spectrum of monarubin B (6) in CDCl ₃ (400 MHz).	25
Figure S21. ¹³ C NMR spectrum of monarubin B (6) in CDCl ₃ (100 MHz).	26
Figure S22. DEPT 135 spectrum of monarubin B (6) in CDCl ₃ (100 MHz).	27
Figure S23. HMQC spectrum of monarubin B (6) in CDCl ₃	28
Figure S24. ¹ H- ¹ H COSY spectrum of monarubin B (6) in CDCl ₃	29
Figure S25. HMBC spectrum of monarubin B (6) in CDCl ₃	30

Figure S26. NOESY spectrum of monarubin B (6) in CDCl ₃	31
Figure S27. ¹ H NMR spectrum of lunatinin (7) in actone-d ₆ (400 MHz).	32
Figure S28. ¹³ C NMR spectrum of lunatinin (7) in actone-d ₆ (100 MHz).	33
Figure S29. ¹ H NMR spectrum of 6,8-dimethoxy-3-methylisocoumarin (8) in CDCl ₃ (400 MHz).	34
Figure S30. ¹³ C NMR spectrum of 6,8-dimethoxy-3-methylisocoumarin (8) in CDCl ₃ (100 MHz).	35
Figure S31. ¹ H NMR spectrum of monasporpurone (9) in CDCl ₃ (400 MHz).	36
Figure S32. ¹³ C NMR spectrum of monasporpurone (9) in CDCl ₃ (100 MHz).	37
Figure S33. ¹ H NMR spectrum of 5-amino-2,6-dimethyl-6-hydroxy-4-(2'-methyl-1-oxobutyl)-3-methoxy-2,4-cyclohexadien-1-one (10) in CDCl ₃ (400 MHz).	38
Figure S34. ¹³ C NMR spectrum of 5-amino-2,6-dimethyl-6-hydroxy-4-(2'-methyl-1-oxobutyl)-3-methoxy-2,4-cyclohexadien-1-one (10) in CDCl ₃ (100 MHz).	39
Figure S35. ¹ H NMR spectrum of phomaligol A (11) in CDCl ₃ (400 MHz).	40
Figure S36. ¹³ C NMR spectrum of phomaligol A (11) in CDCl ₃ (100 MHz).	41
Figure S37. ¹ H NMR spectrum of monascuspiloin (12) in CDCl ₃ (400 MHz).	42
Figure S38. ¹³ C NMR spectrum of monascuspiloin (12) in CDCl ₃ (100 MHz).	43
Figure S39. HR-(+) ESI-MS spectrum of monarubin C (13).	44
Figure S40. ¹ H NMR spectrum of monarubin C (13) in CDCl ₃ (600 MHz).	45

Figure S41. ^{13}C NMR spectrum of monarubin C (13) in CDCl_3 (150 MHz).	46
Figure S42. DEPT 135 spectrum of monarubin C (13) in CDCl_3 (150 MHz).	47
Figure S43. HMQC spectrum of monarubin C (13) in CDCl_3	48
Figure S44. ^1H - ^1H COSY spectrum of monarubin C (13) in CDCl_3	49
Figure S45. HMBC spectrum of monarubin C (13) in CDCl_3	50
Figure S46. NOESY spectrum of monarubin C (13) in CDCl_3	51
Figure S47. The most stable conformers of 11 <i>S</i> - 6 calculated at the B3LYP/6-31+G(d) level. Relative populations are in parentheses.	52
Figure S48. The most stable conformers of 11 <i>R</i> - 6 calculated at the B3LYP/6-31+G(d) level. Relative populations are in parentheses.	53
Figure S49. The most stable conformers of 3 <i>S</i> ,6 <i>R</i> ,7 <i>S</i> ,11 <i>S</i> ,17 <i>R</i> - 13 calculated at the B3LYP/6-31+G(d) level. Relative populations are in parentheses.	54
Figure S50. The most stable conformers of 3 <i>S</i> ,6 <i>R</i> ,7 <i>S</i> ,11 <i>S</i> ,17 <i>S</i> - 13 calculated at the B3LYP/6-31+G(d) level. Relative populations are in parentheses.	55
Figure S51. The most stable conformers of 3 <i>R</i> ,6 <i>S</i> ,7 <i>R</i> ,11 <i>R</i> ,17 <i>S</i> - 13 calculated at the B3LYP/6-31+G(d) level. Relative populations are in parentheses.	56
Figure S52. The most stable conformers of 3 <i>R</i> ,6 <i>S</i> ,7 <i>R</i> ,11 <i>R</i> ,17 <i>R</i> - 13 calculated at the B3LYP/6-31+G(d) level. Relative populations are in parentheses.	57
Figure S53. The most stable conformers of 11 <i>S</i> - 3 calculated at the B3LYP/6-31+G(d) level. Relative populations are in parentheses.	58

Figure S54. The most stable conformers of 11 <i>R</i> - 3 calculated at the B3LYP/6-31+G(d) level. Relative populations are in parentheses.	59
Table S1. X-ray Crystallography Data for 4	60
Table S2. The hepatocellular carcinoma cell line HepG2 activity of manorubin B (6).....	62
Table S3. The hepatocellular carcinoma cell line QGY7701 activity of manorubin B (6).....	62
Table S4. The nasopharyngeal carcinoma cell line SUNE1 activity of lunatinin (7)	63
Table S5. The hepatocellular carcinoma cell line HepG2 activity of lunatinin (7).....	63
Table S6. The hepatocellular carcinoma cell line QGY7701 activity of lunatinin (7)	63

1903A1060-1 #3 RT: 0.03 AV: 1 NL: 2.94E8
T: FTMS + c ESI Full ms [100.0000-1000.0000]



SPECTRUM-simulation :

m/z	Theo. Mass	Delta (ppm)	RDB equiv.	Composition
207.14923	207.14919	0.19	4.5	C12 H19 O N2

Figure S1. HR-(+) ESI-MS spectrum of monarubin A (**1**).

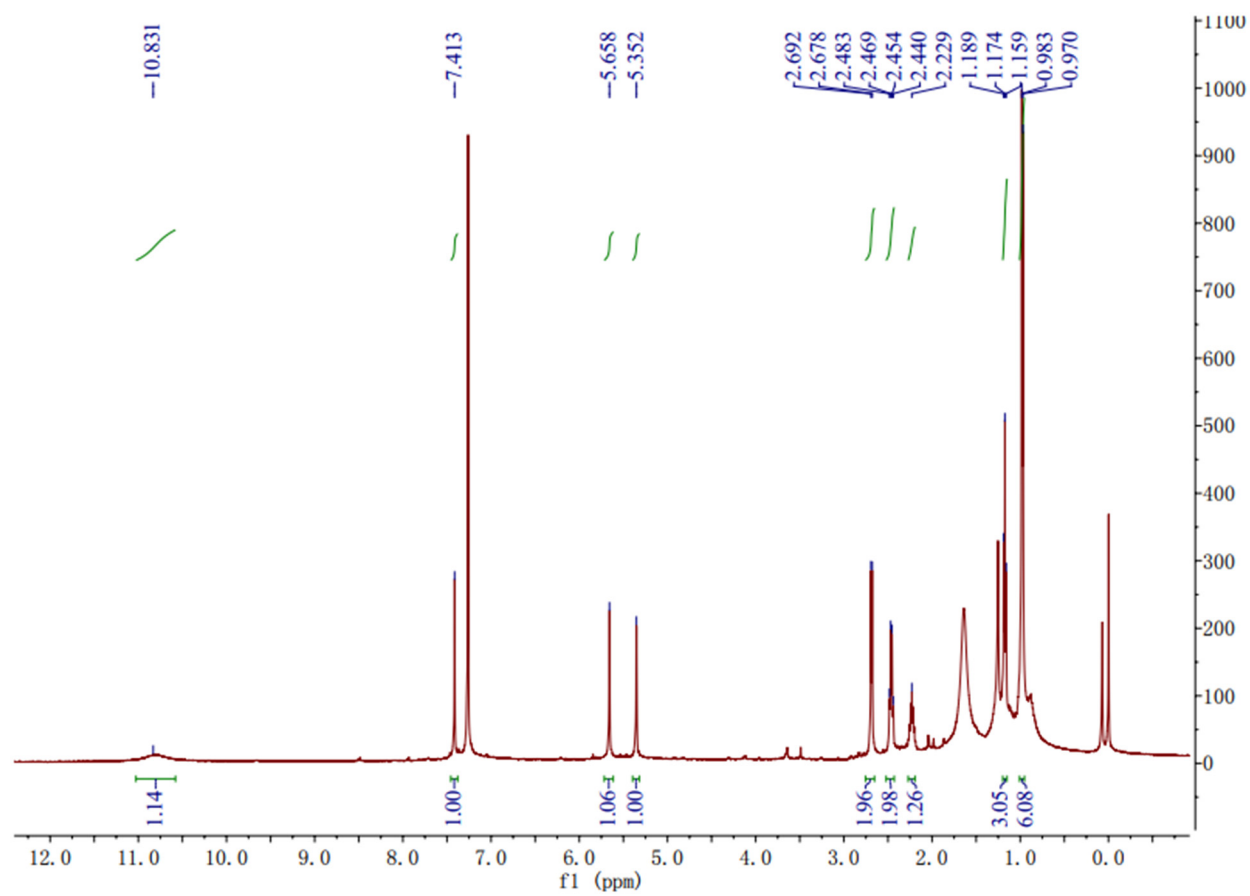


Figure S2. ^1H NMR spectrum of monarubin A (**1**) in CDCl_3 (500 MHz).

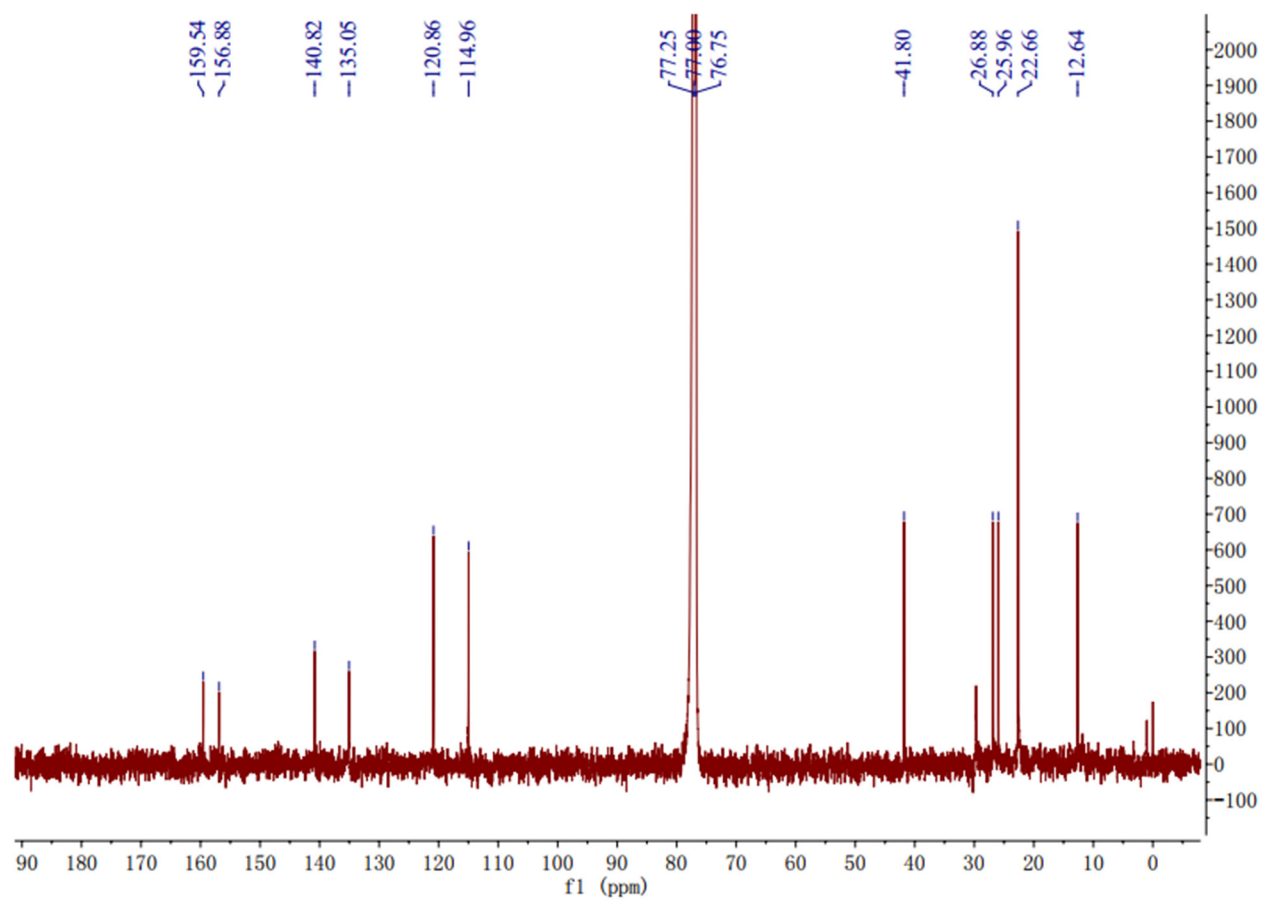


Figure S3. ^{13}C NMR spectrum of monarubin A (1) in CDCl_3 (125 MHz).

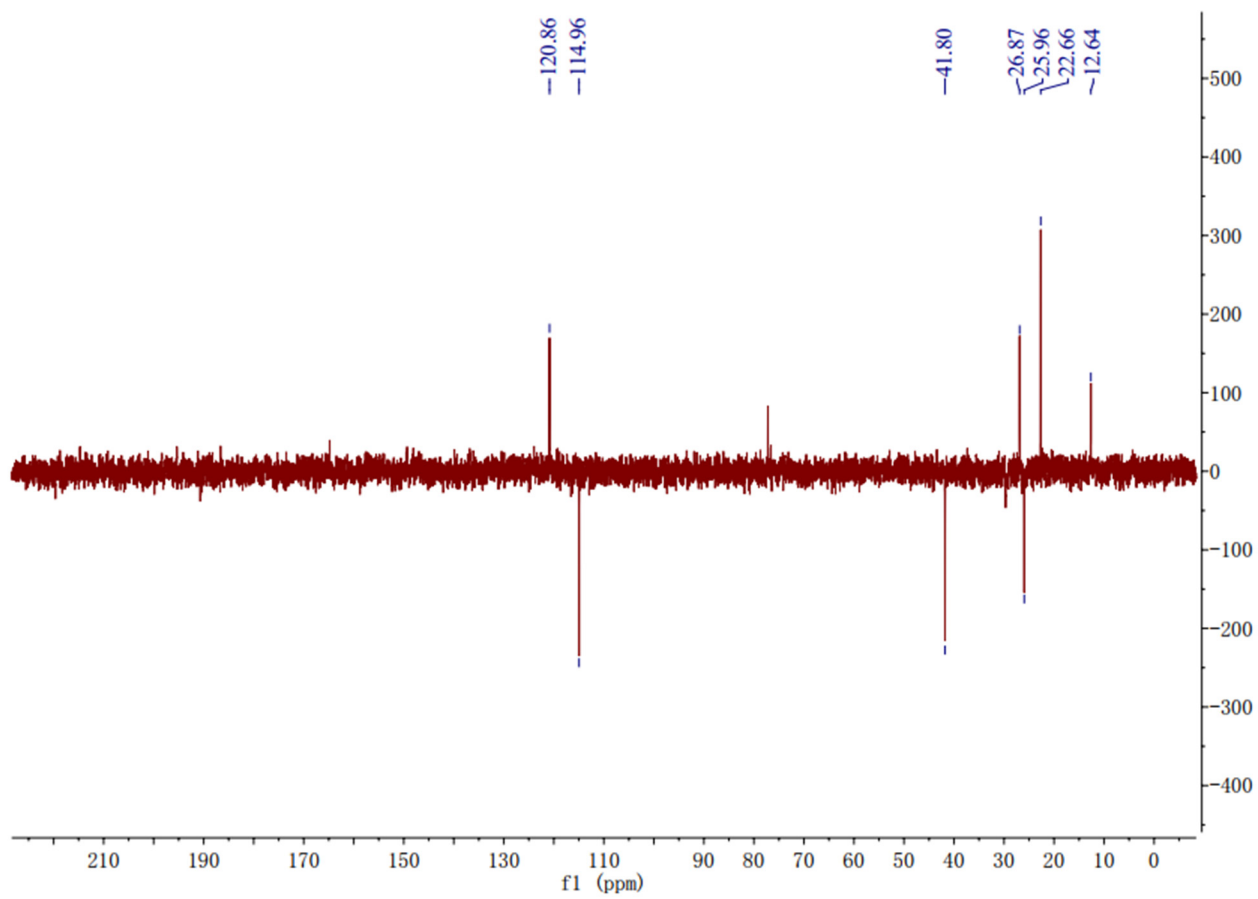


Figure S4. DPET 135 spectrum of monarubin A (**1**) in CDCl₃ (125 MHz).

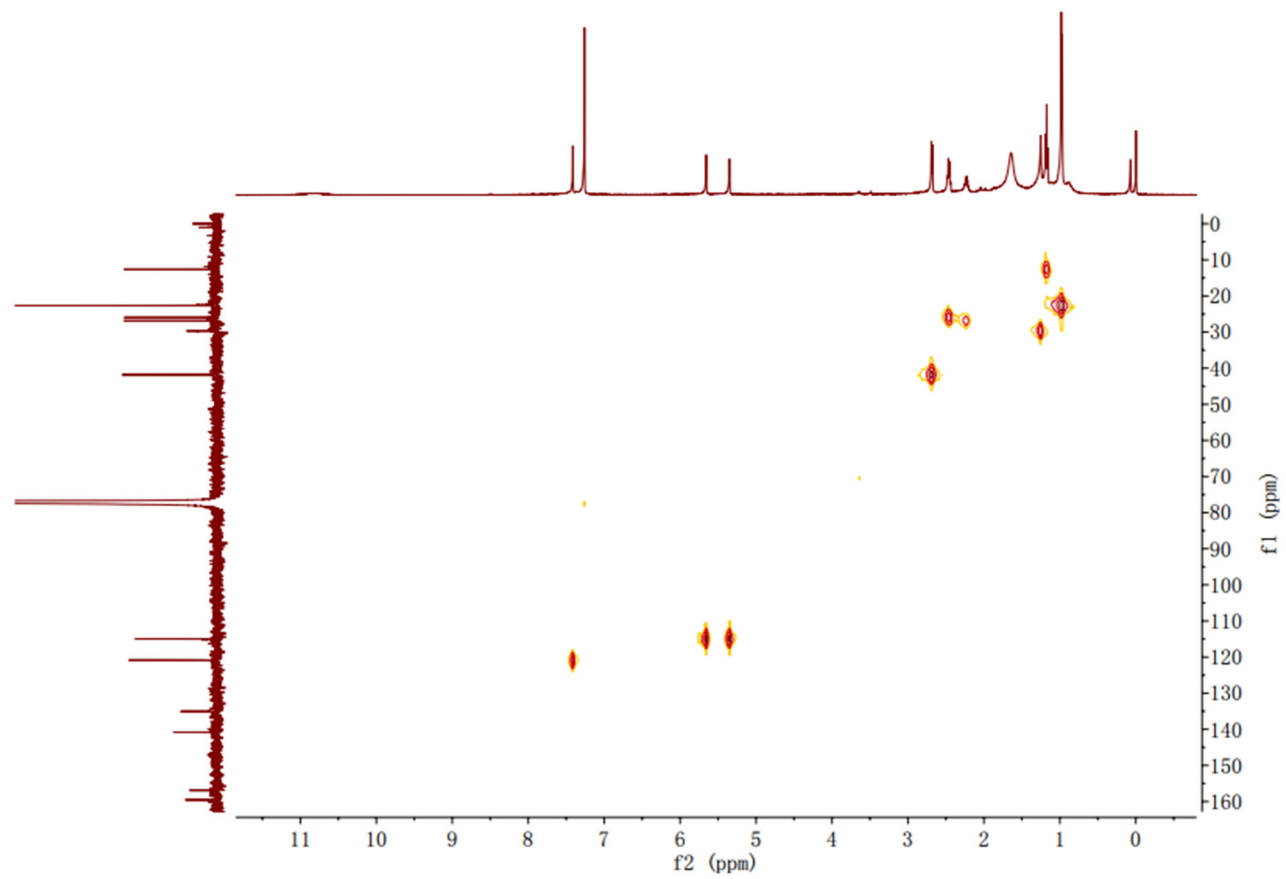


Figure S5. HMQC spectrum of monarubin A (**1**) in CDCl₃.

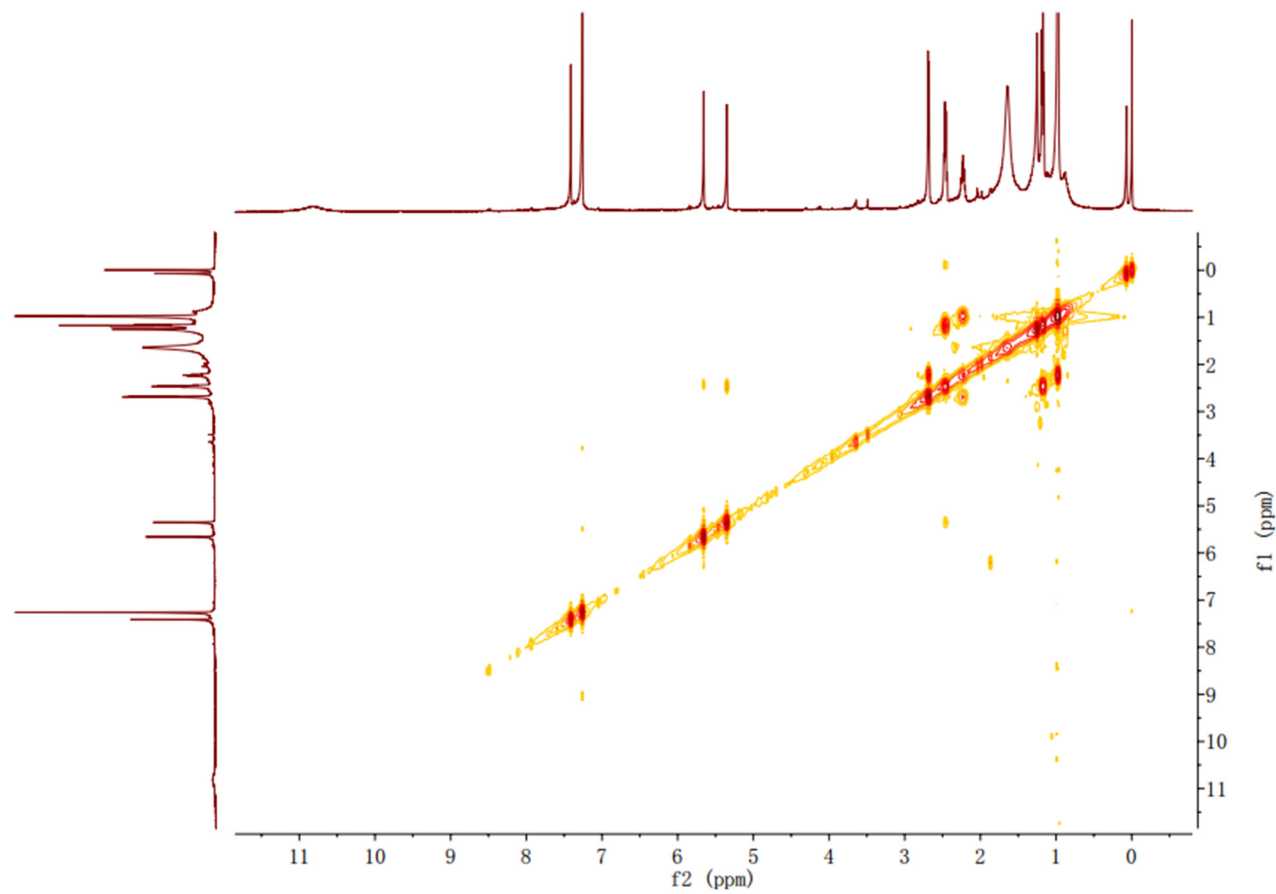


Figure S6. ^1H - ^1H COSY spectrum of monarubin A (**1**) in CDCl_3 .

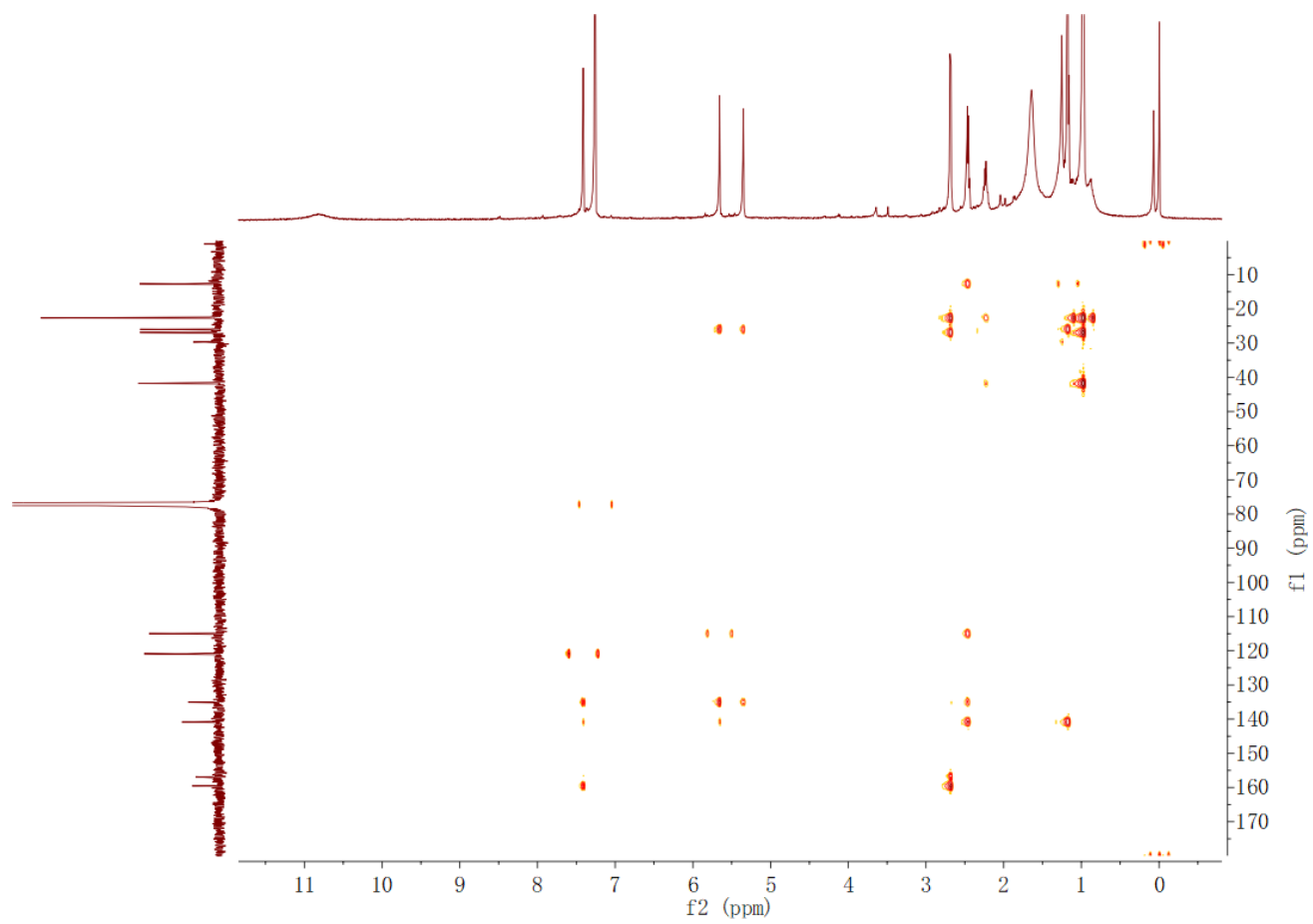


Figure S7. HMBC spectrum of monarubin A (**1**) in CDCl₃.

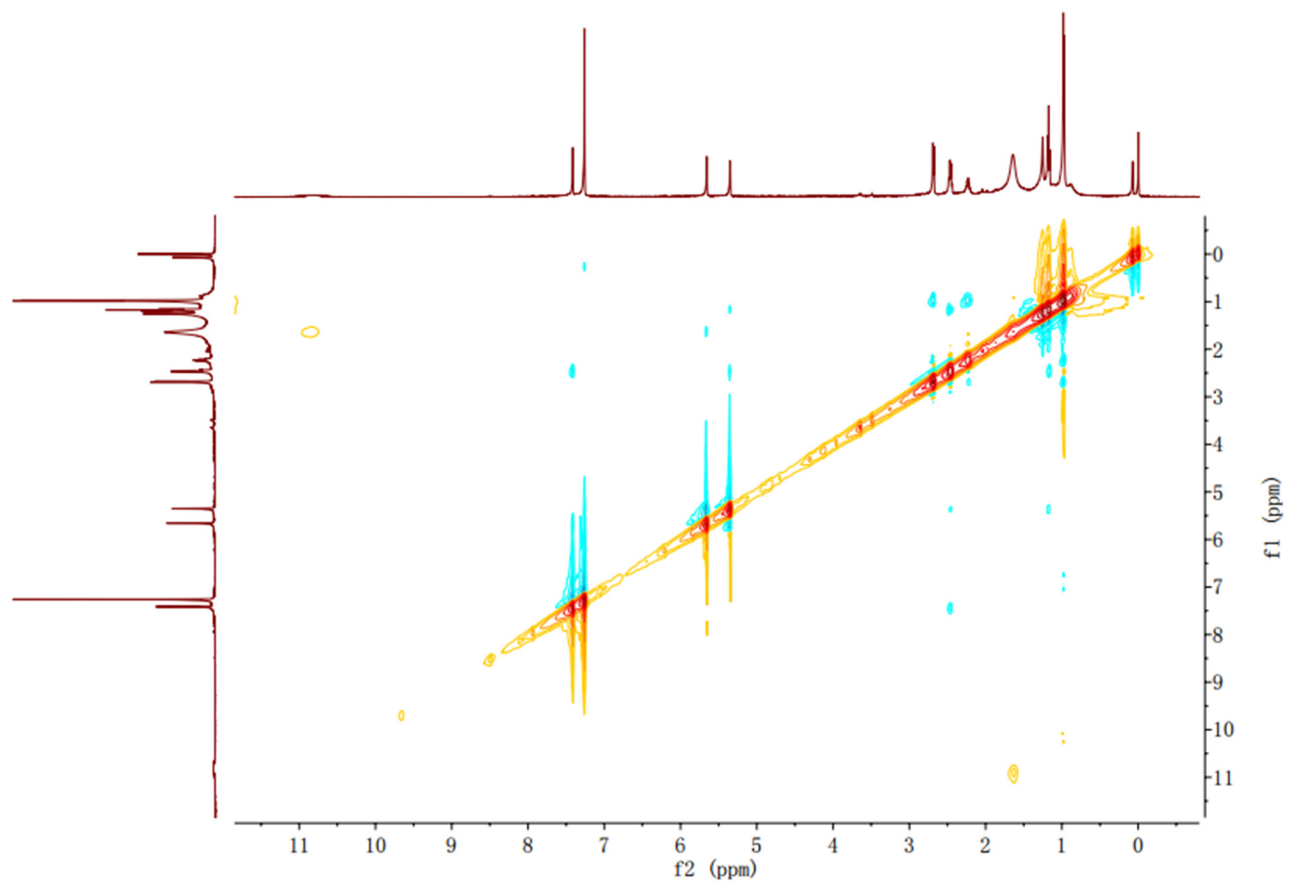


Figure S8. NOESY spectrum of monarubin A (**1**) in CDCl_3 .

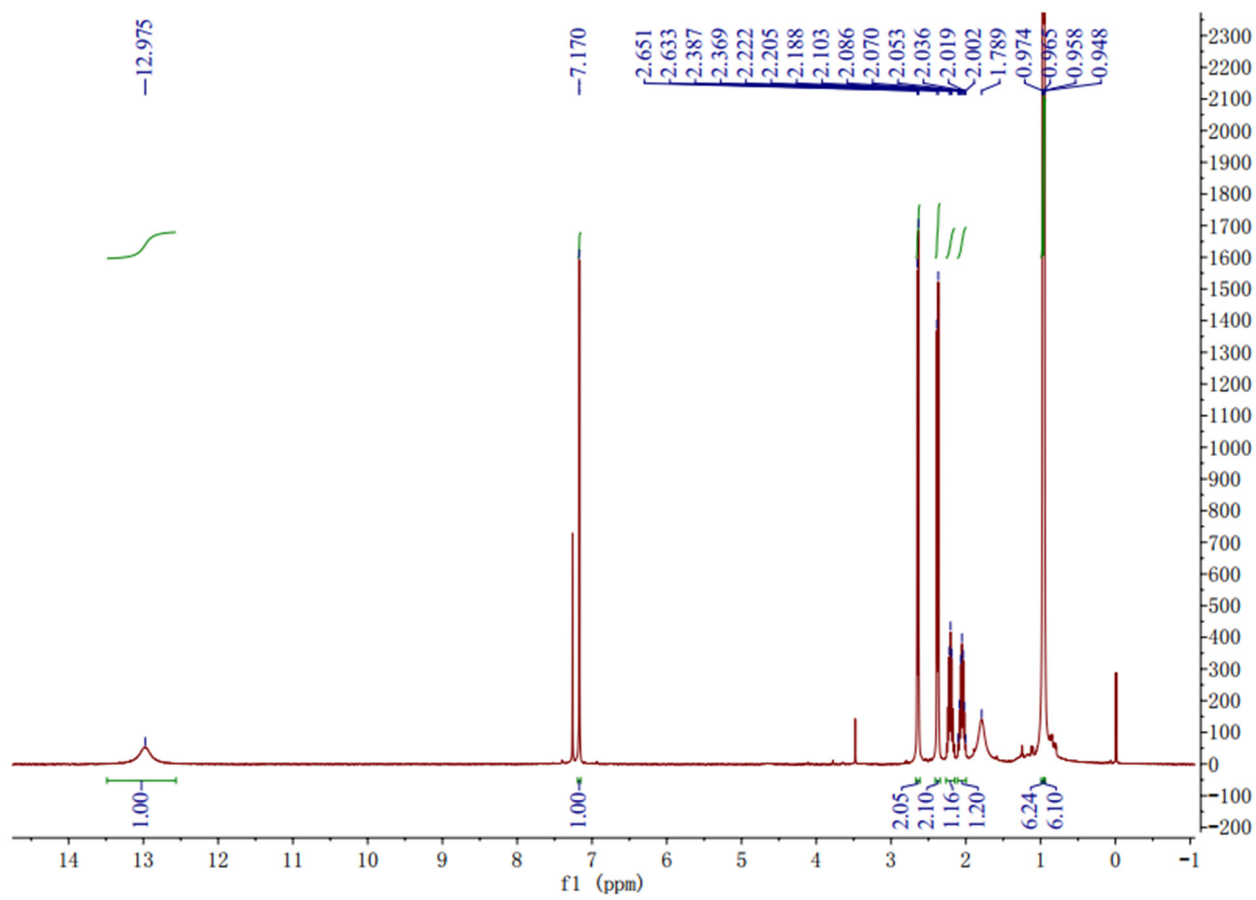


Figure S9. ^1H NMR spectrum of 3,6-diisobutyl-2(1H)-pyrazinone (**2**) in CDCl_3 (400 MHz).

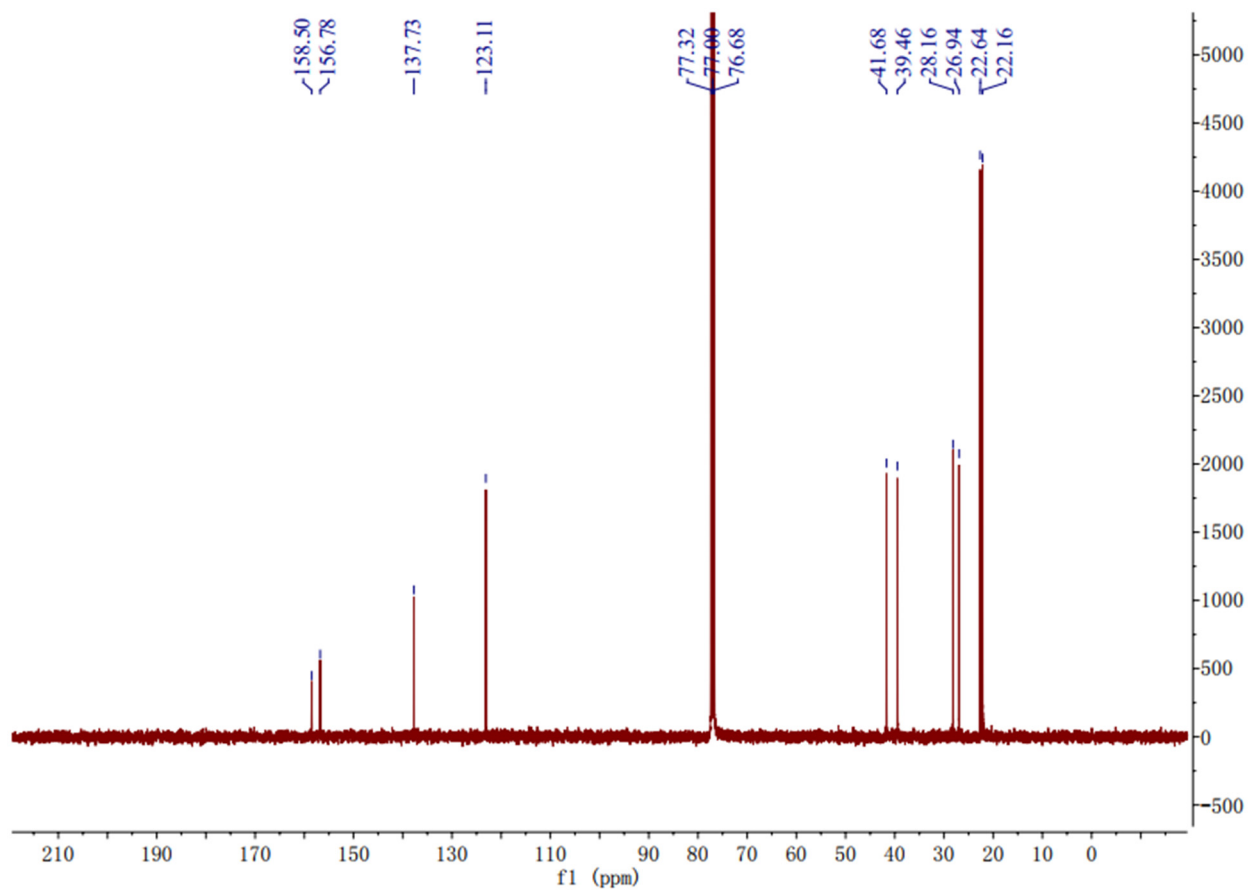
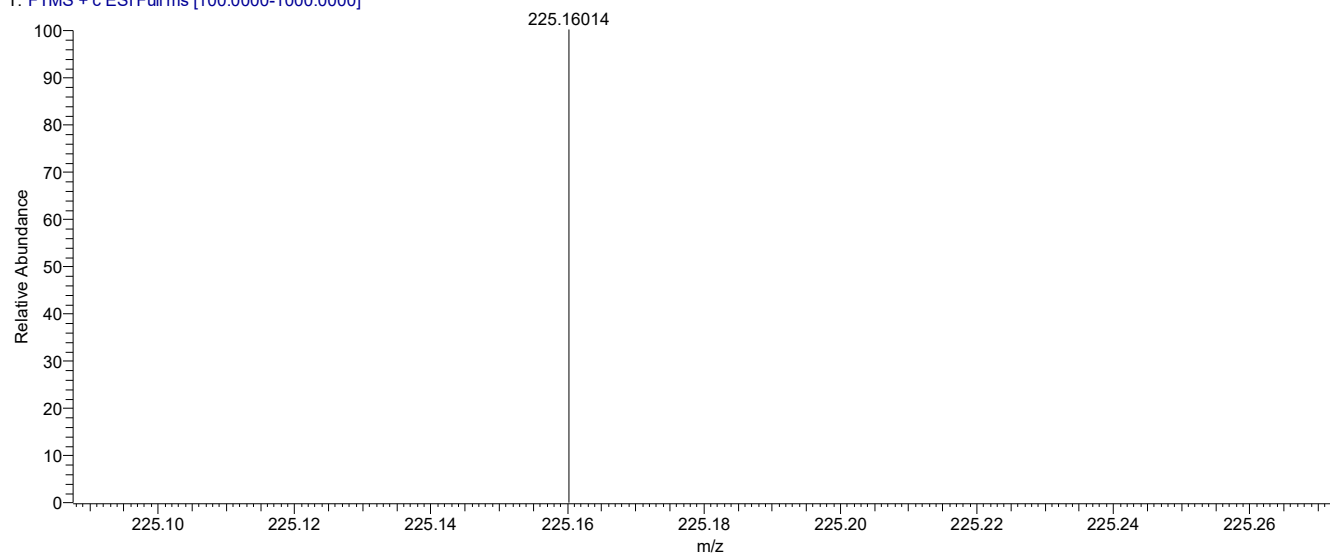


Figure S10. ¹³C NMR spectrum of 3,6-diisobutyl-2(1*H*)-pyrazinone (**2**) in CDCl₃ (100 MHz).

1910a0540-1-57min #7 RT: 0.06 AV: 1 NL: 1.29E8
T: FTMS + c ESI Full ms [100.0000-1000.0000]



SPECTRUM-simulation :

m/z	Theo. Mass	Delta (ppm)	RDB equiv.	Composition
225.16019	225.15975	1.93	3.5	C12 H21 O2 N2

Figure S11. HR-(+) ESI-MS spectrum of deoxyhydroxyaspergillic acid (**3**).

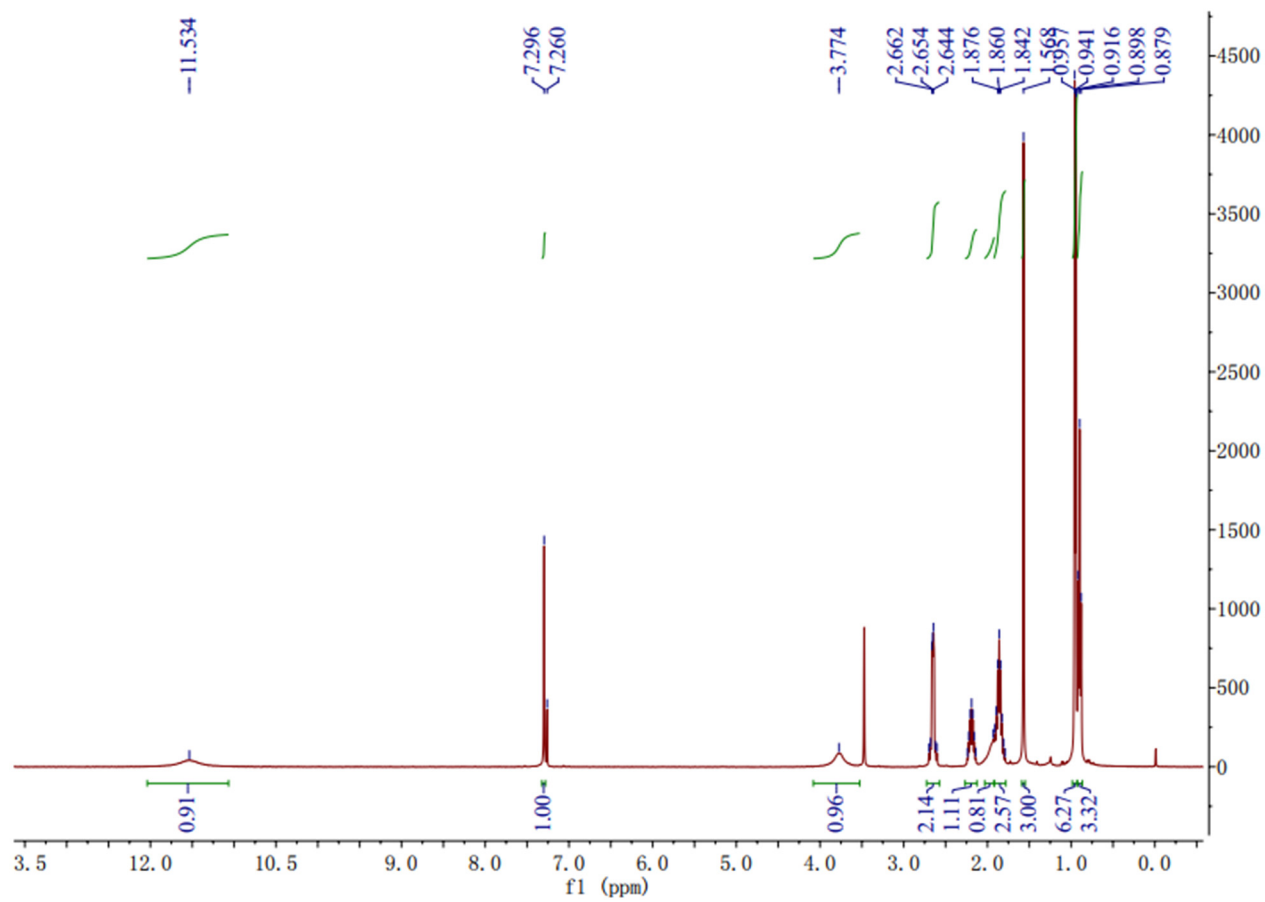


Figure S12. ^1H NMR spectrum of deoxyhydroxyaspergillic acid (**3**) in CDCl_3 (400 MHz).

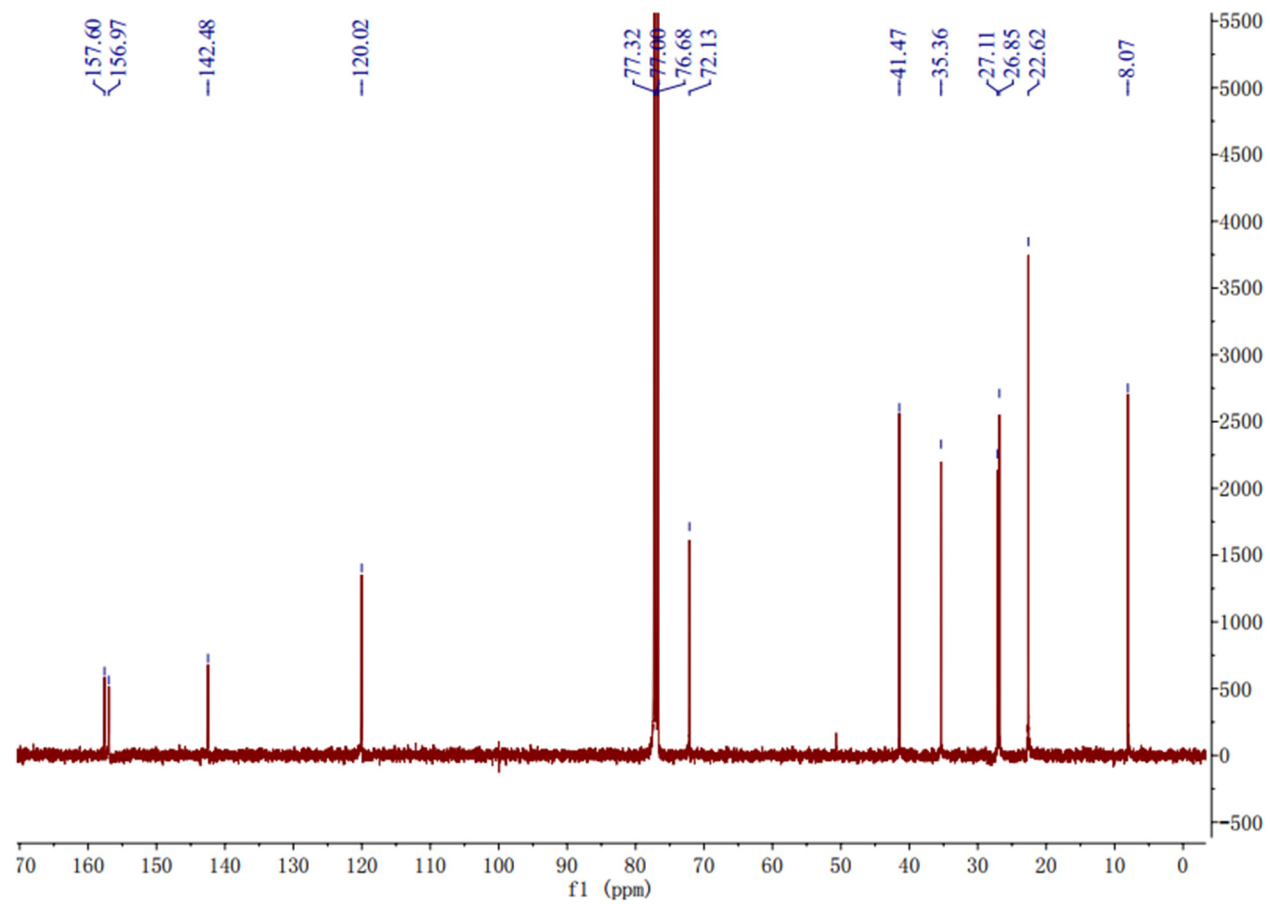
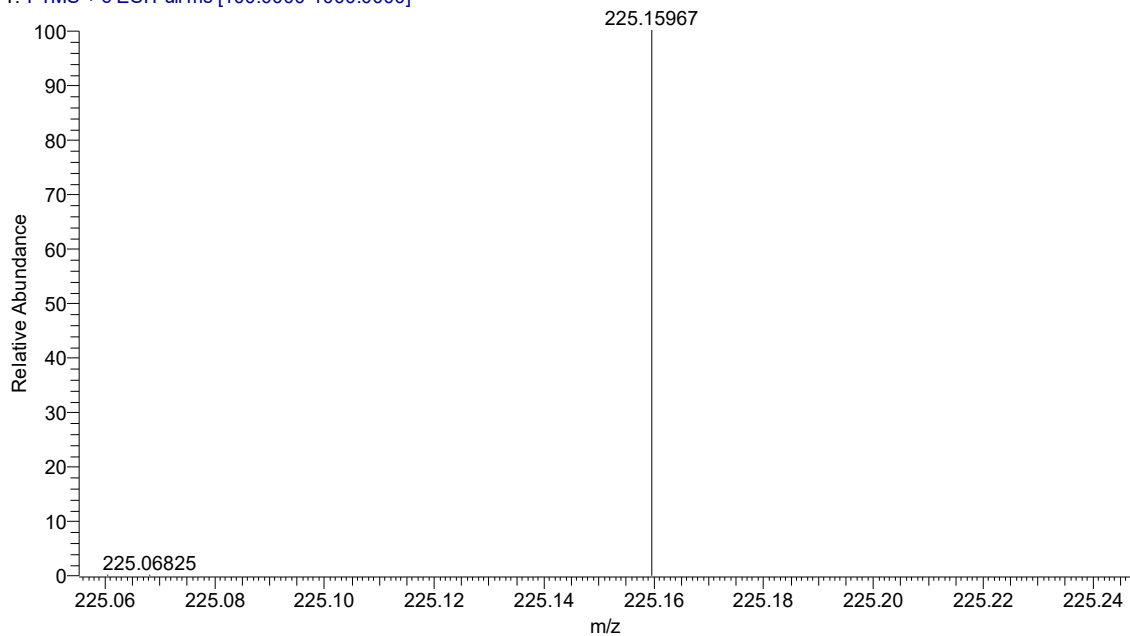


Figure S13. ^{13}C NMR spectrum of deoxyhydroxyaspergillilic acid (**3**) in CDCl_3 (100 MHz).

1910a0540-2 #9 RT: 0.08 AV: 1 NL: 3.84E7
T: FTMS + c ESI Full ms [100.0000-1000.0000]



SPECTRUM-simulation :

m/z	Theo. Mass	Delta (ppm)	RDB equiv.	Composition
225.15967	225.15975	-0.37	3.5	C12 H21 O2 N2

Figure S14. HR-(+) ESI-MS spectrum of 2-hydroxy-6-(1-hydroxy-1-methylpropyl) 3-*sec*-butylpyrazine (**4**).

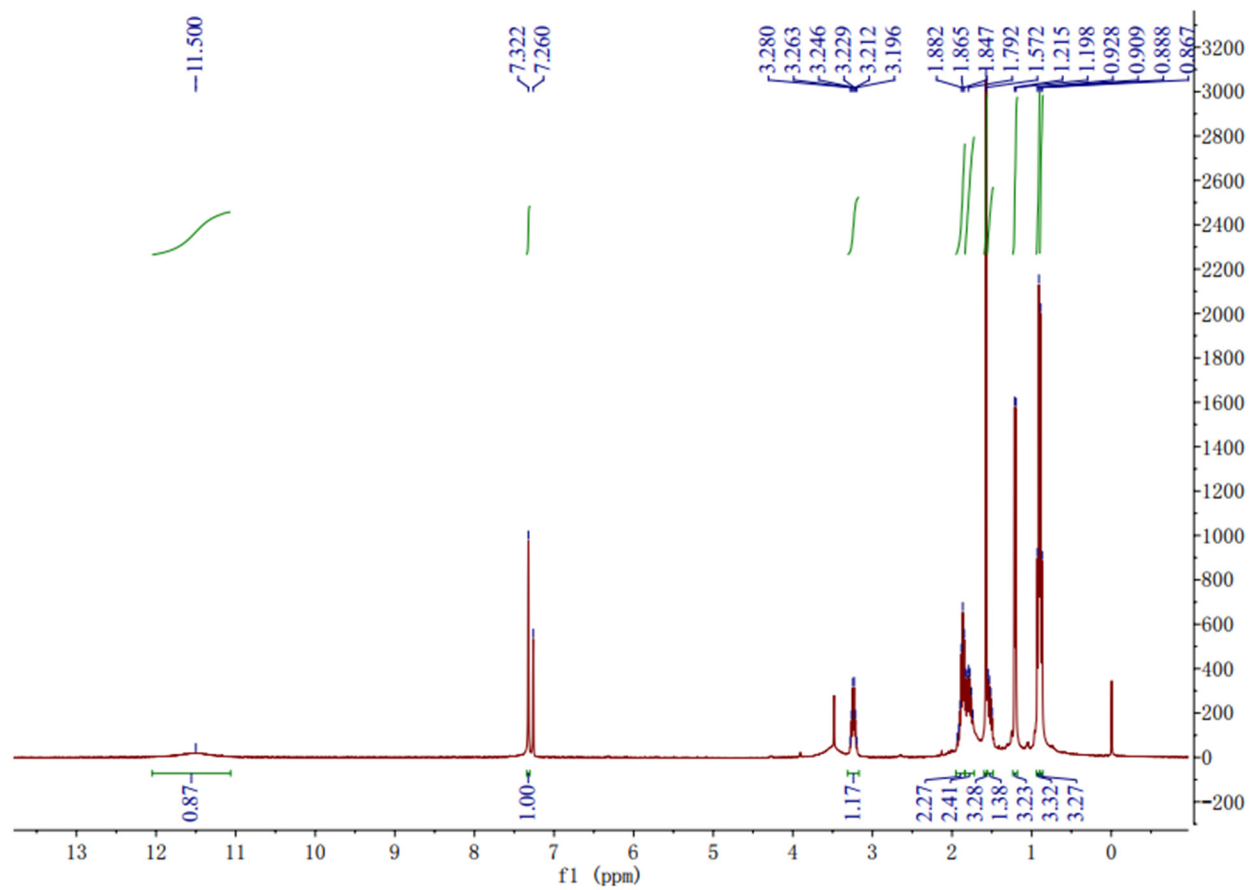


Figure S15. ^1H NMR spectrum of 2-hydroxy-6-(1-hydroxy-1-methylpropyl) 3-*sec*-butylpyrazine (**4**) in CDCl_3 (400 MHz).

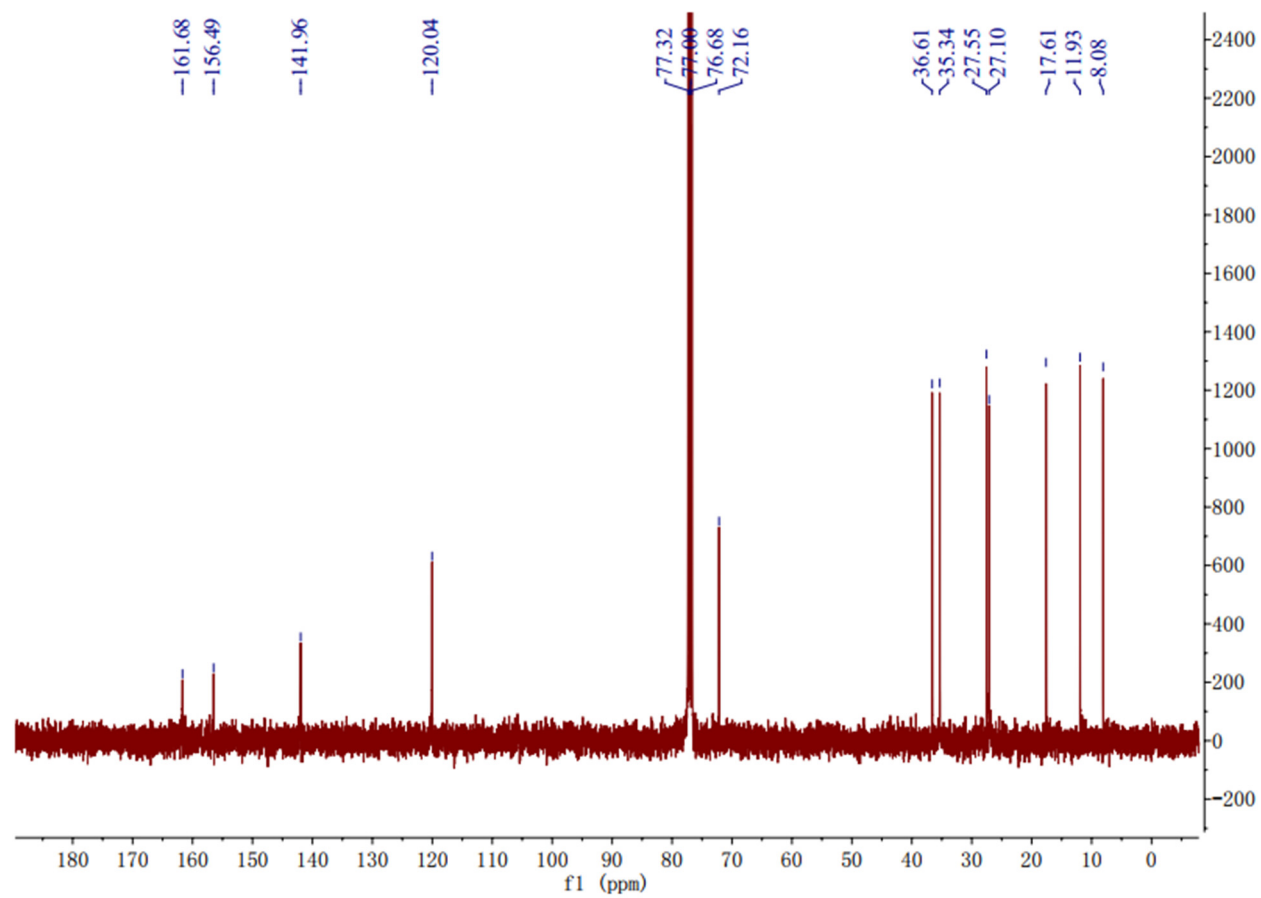


Figure S16. ¹³C NMR spectrum of 2-hydroxy-6-(1-hydroxy-1-methylpropyl) 3-*sec*-buthylpyrazine (**4**) in CDCl₃ (100 MHz).

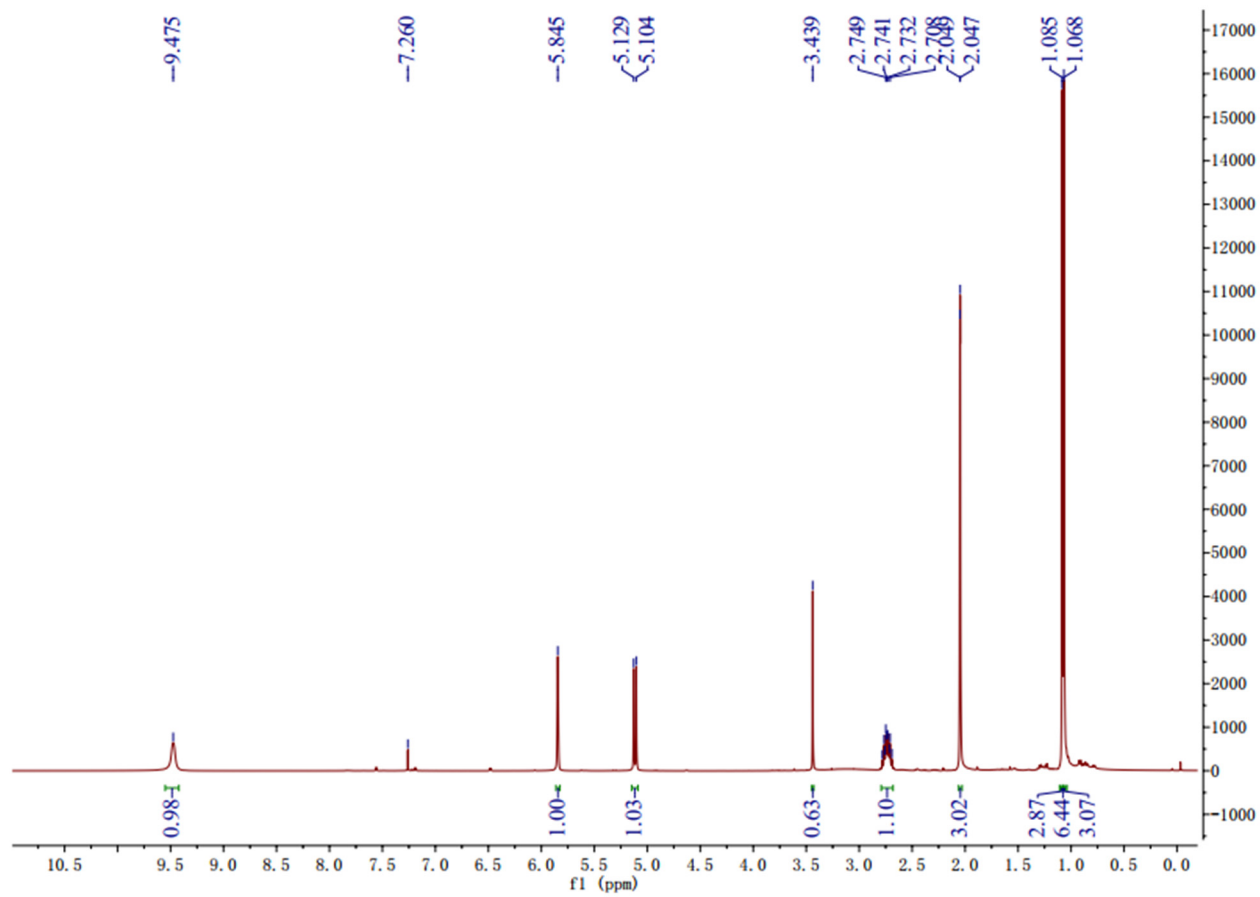


Figure S17. ¹H NMR spectrum of pulchellalactam (**5**) in CDCl₃ (400 MHz).

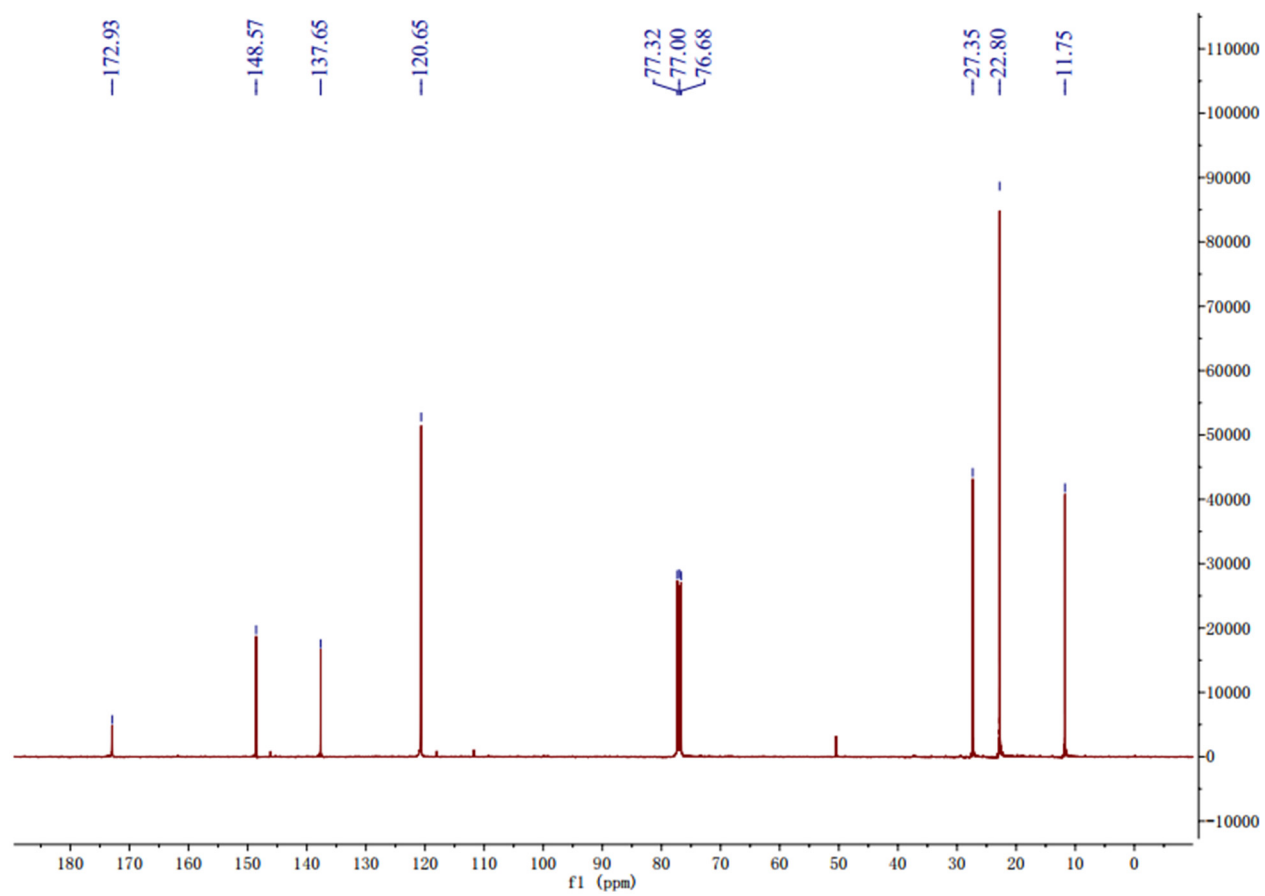
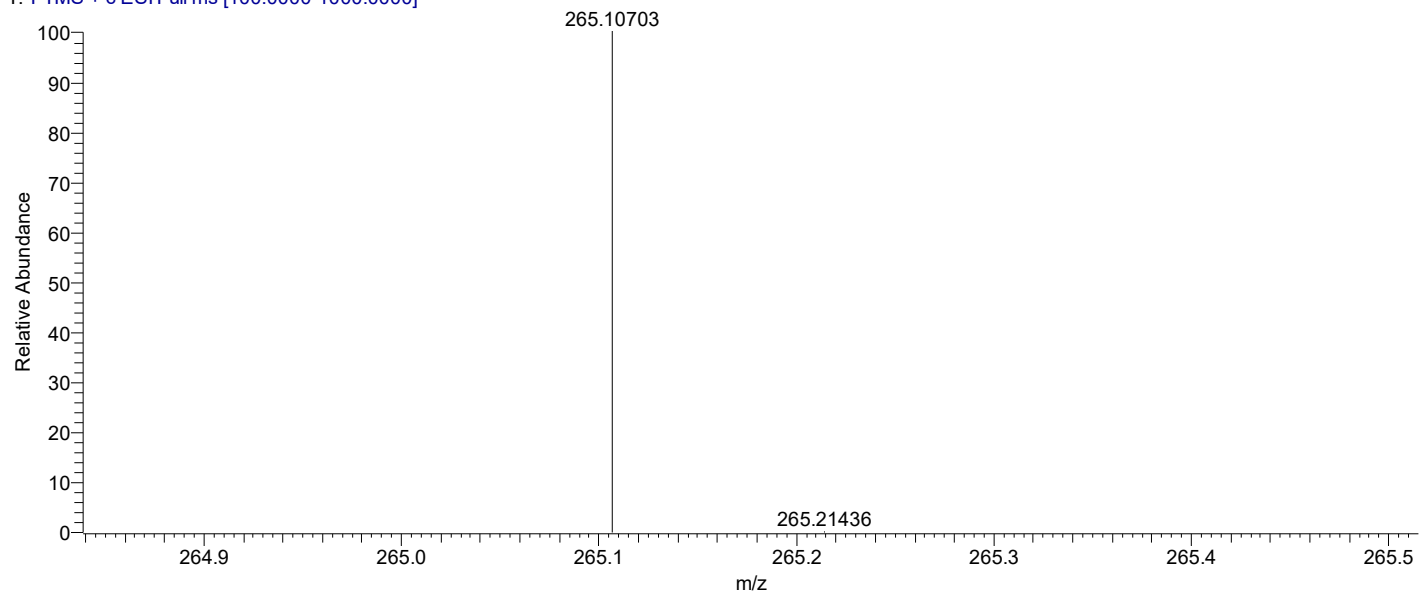


Figure S18. ^{13}C NMR spectrum of pulchellalactam (**5**) in CDCl_3 (100 MHz).

1905A0443-1 #5 RT: 0.05 AV: 1 NL: 2.04E8
T: FTMS + c ESI Full ms [100.0000-1000.0000]



SPECTRUM - simulation :

m/z	Theo. Mass	Delta (ppm)	RDB equiv.	Composition
265.10703	265.10705	-0.08	6.5	C14 H17 O5

Figure S19. HR-(+) ESI-MS spectrum of monarubin B (6).

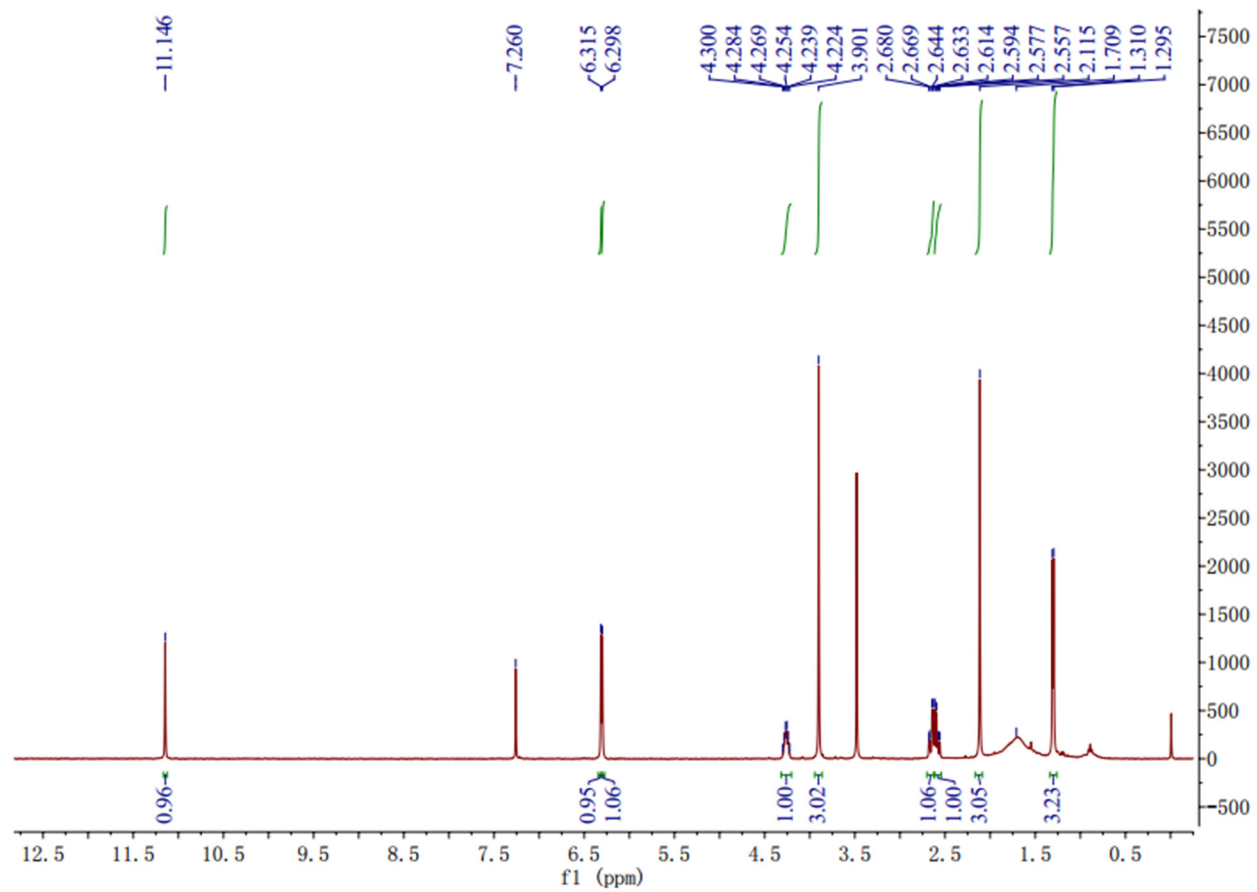


Figure S20. ^1H NMR spectrum of monarubin B (**6**) in CDCl_3 (400 MHz).

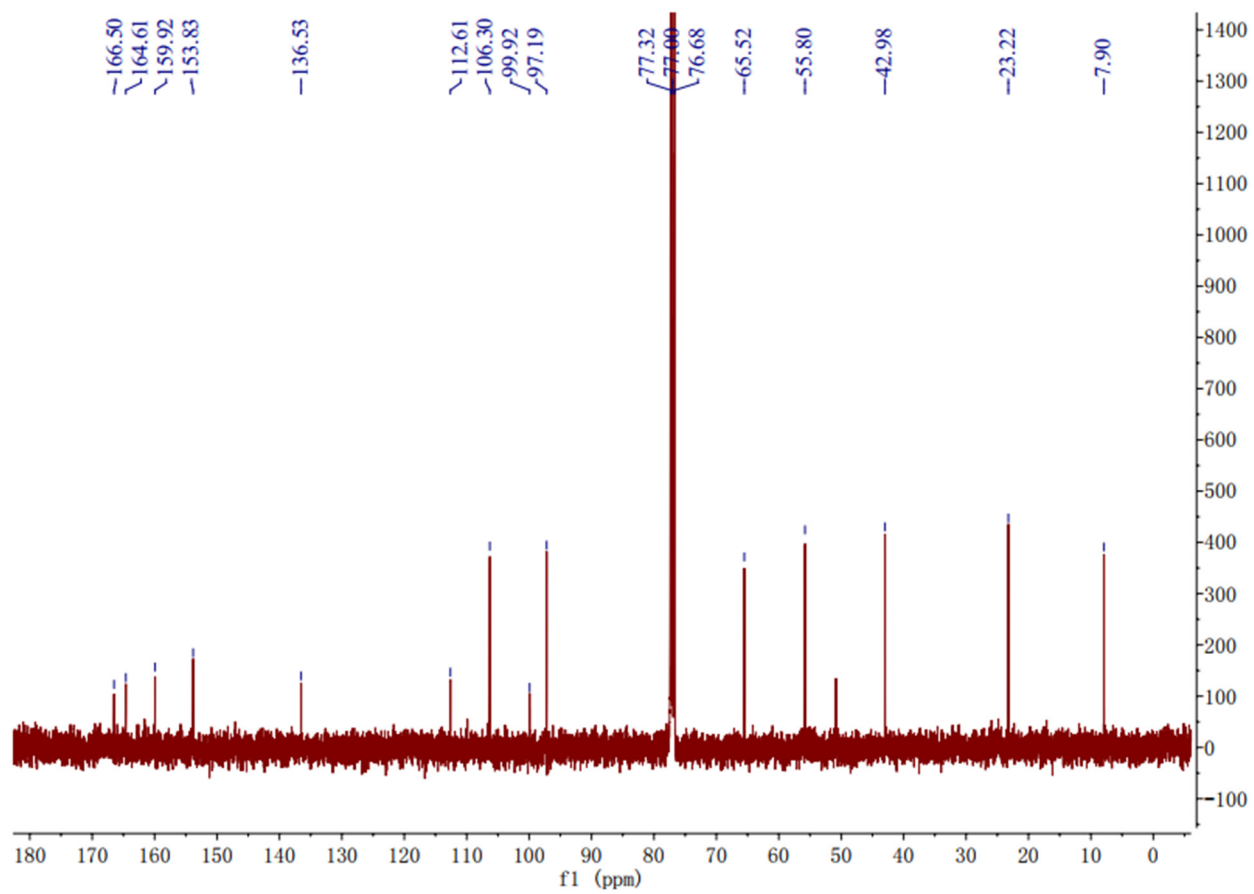


Figure S21. ^{13}C NMR spectrum of monarubin B (**6**) in CDCl_3 (100 MHz).

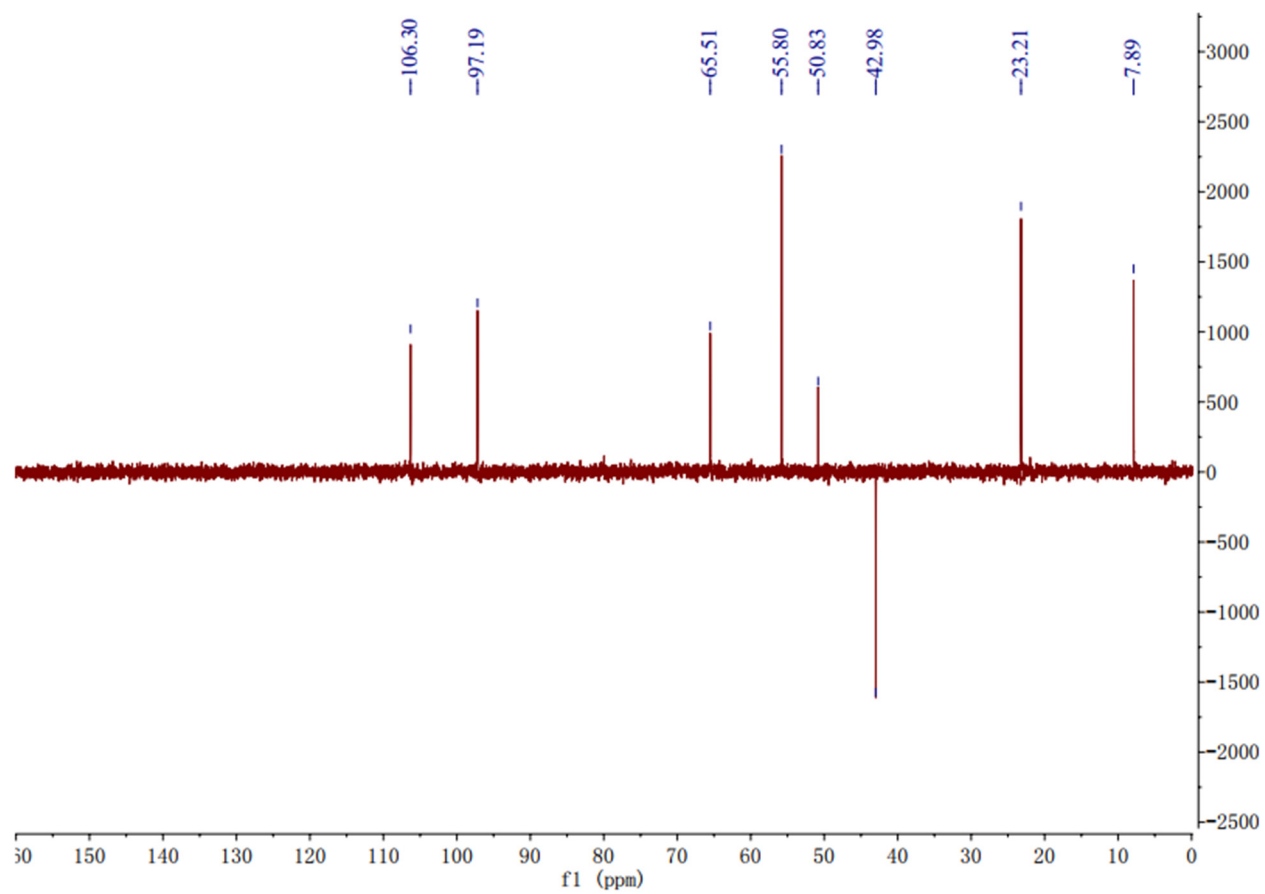


Figure S22. DEPT 135 spectrum of monarubin B (**6**) in CDCl₃ (100 MHz).

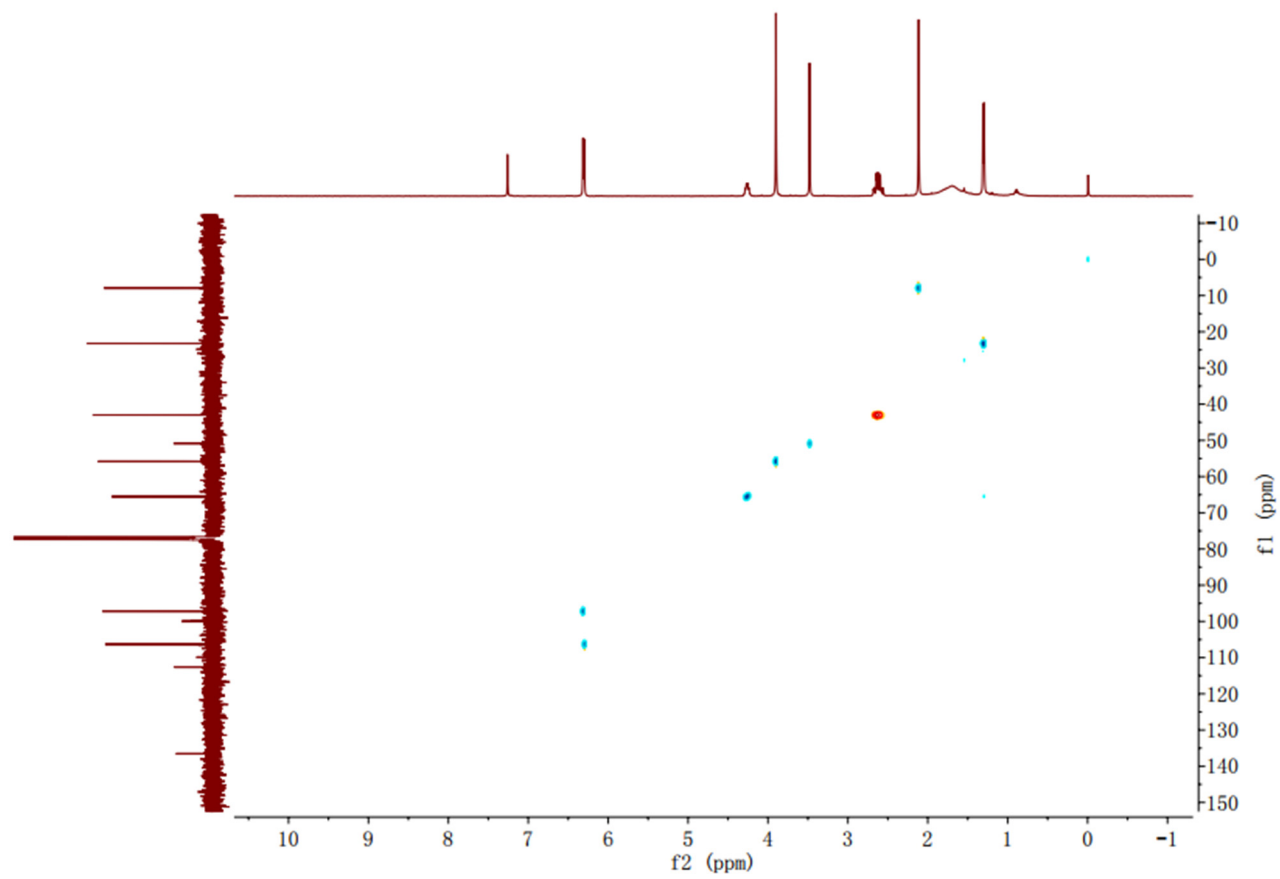


Figure S23. HMQC spectrum of monarubin B (**6**) in CDCl₃.

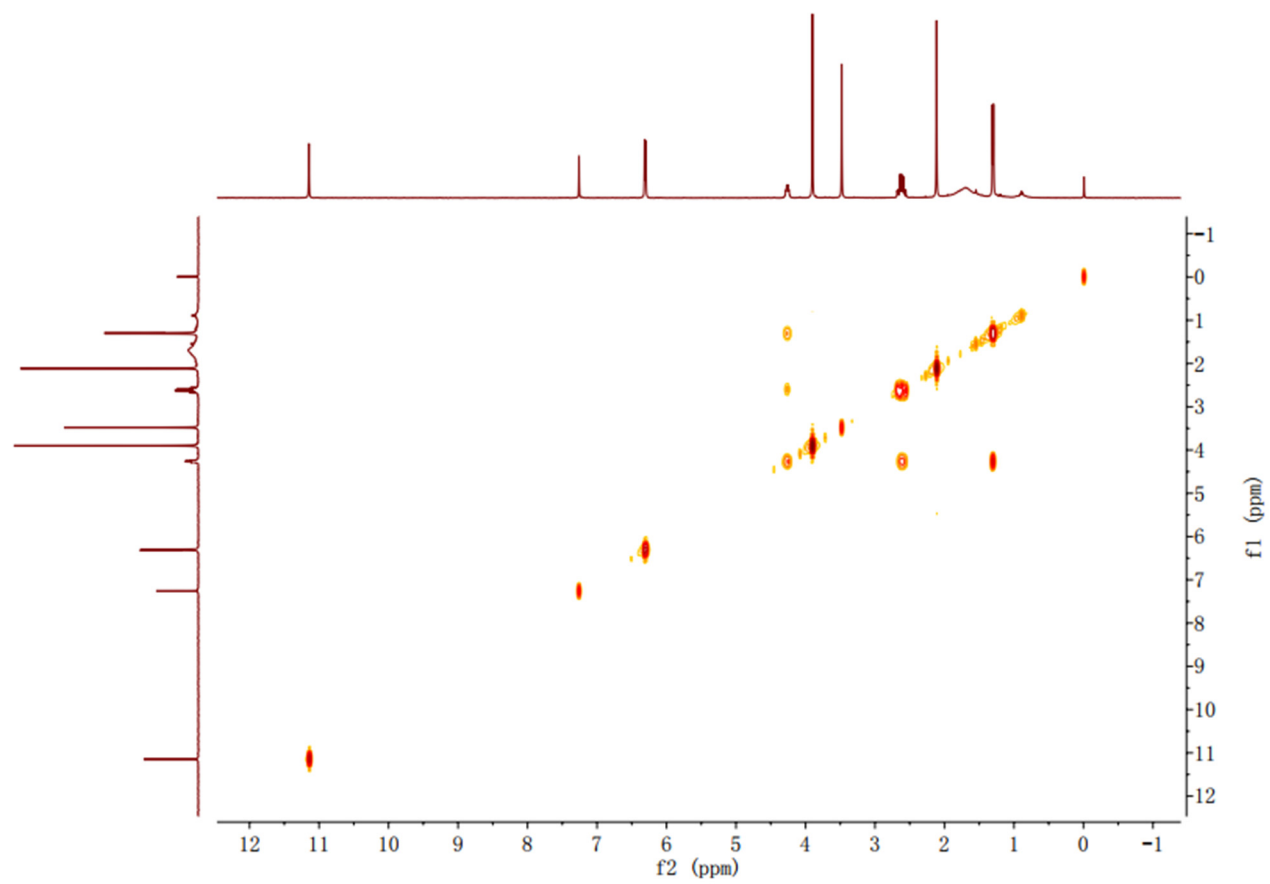


Figure S24. ^1H - ^1H COSY spectrum of monarubin B (**6**) in CDCl_3 .

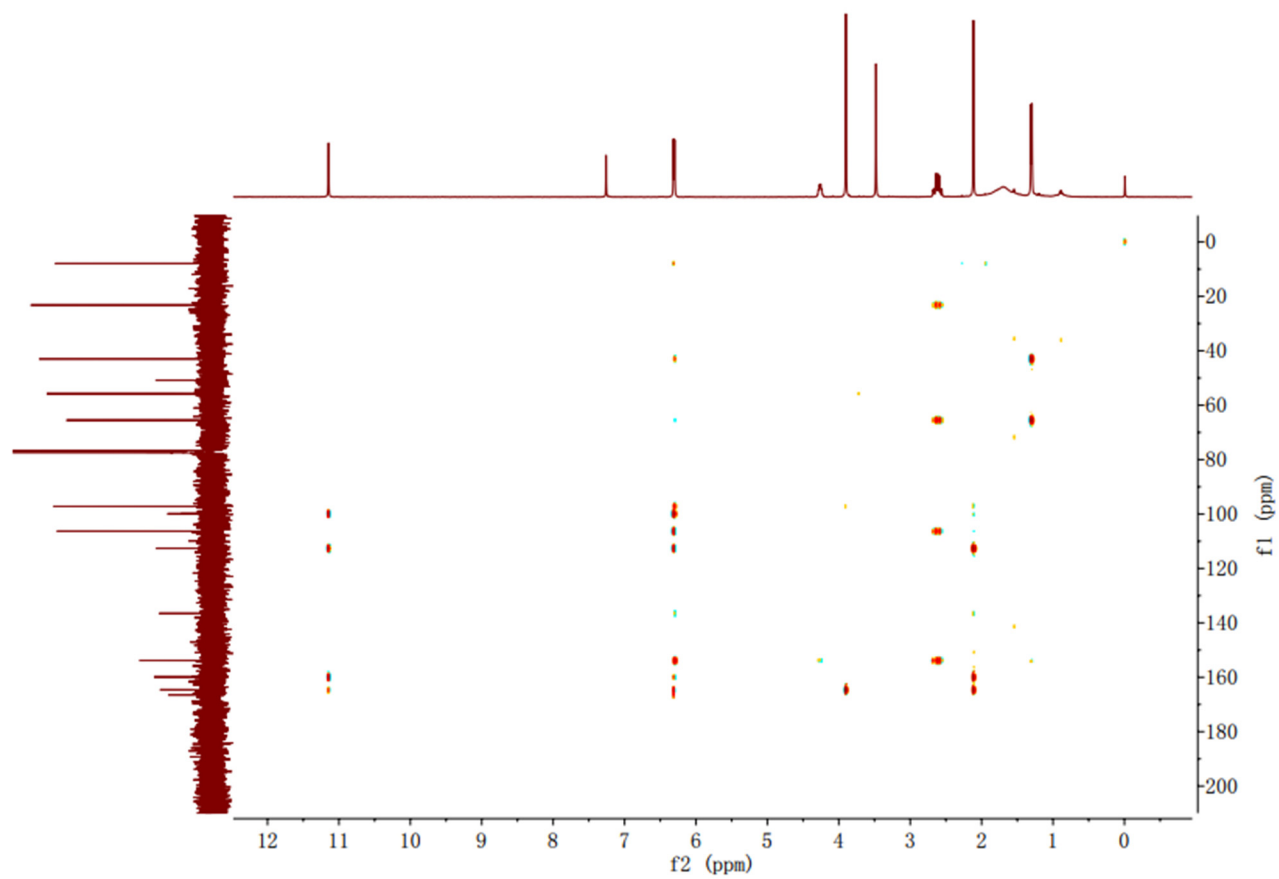


Figure S25. HMBC spectrum of monarubin B (**6**) in CDCl₃.

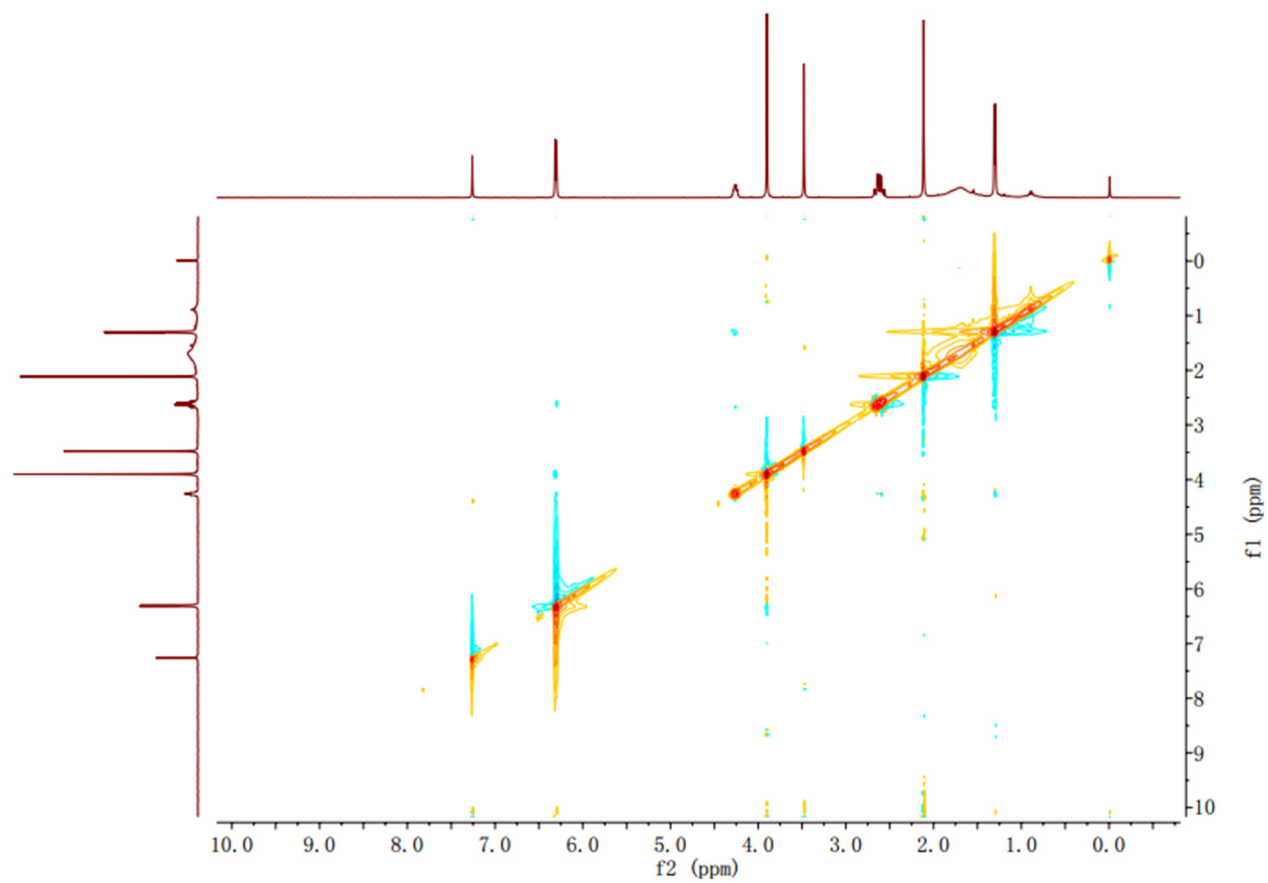


Figure S26. NOESY spectrum of monarubin B (**6**) in CDCl_3 .

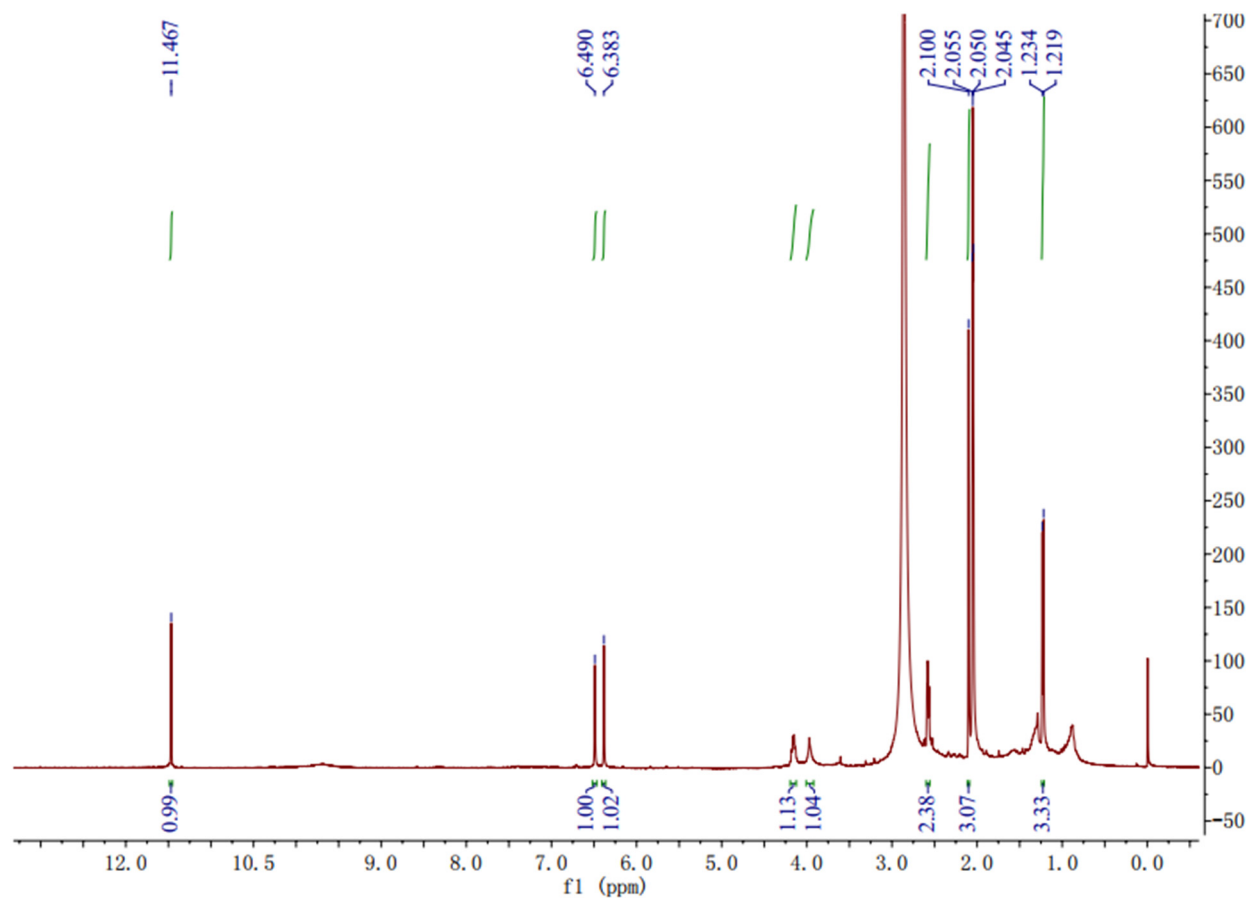


Figure S27. ¹H NMR spectrum of lunatinin (7) in actone-d₆ (400 MHz).

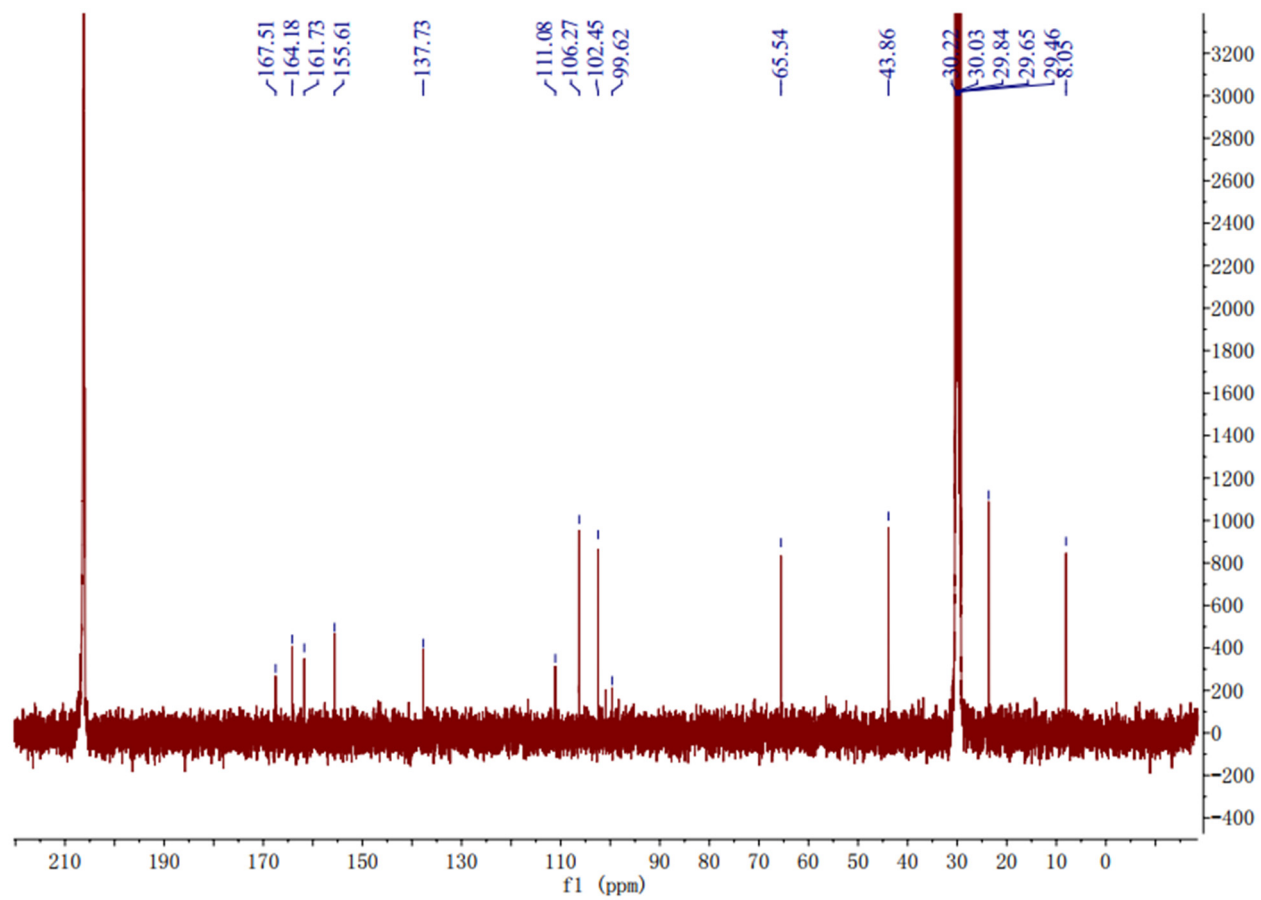


Figure S28. ^{13}C NMR spectrum of lunatinin (7) in actone-d_6 (100 MHz).

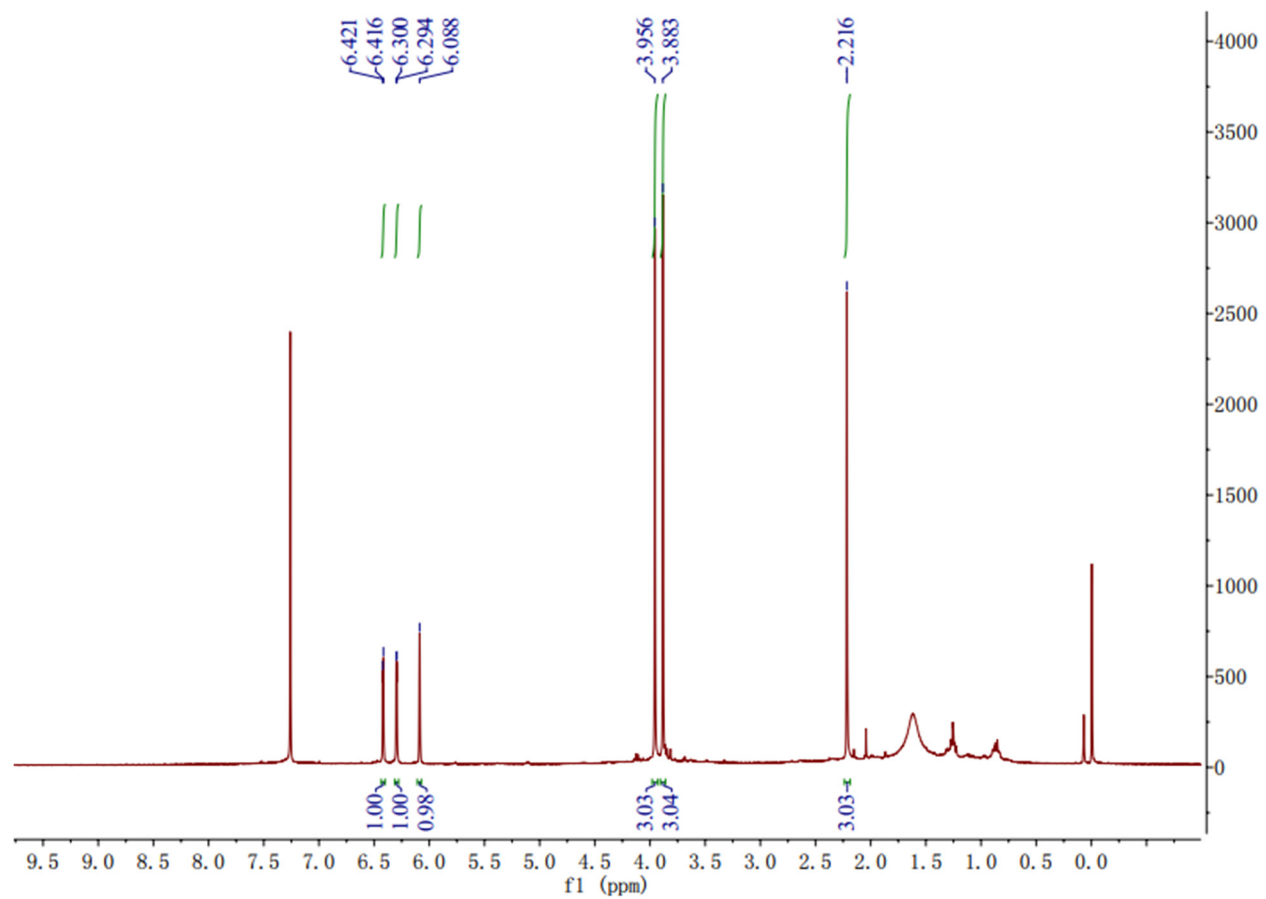


Figure S29. ¹H NMR spectrum of 6,8-dimethoxy-3-methylisocoumarin (**8**) in CDCl₃ (400 MHz).

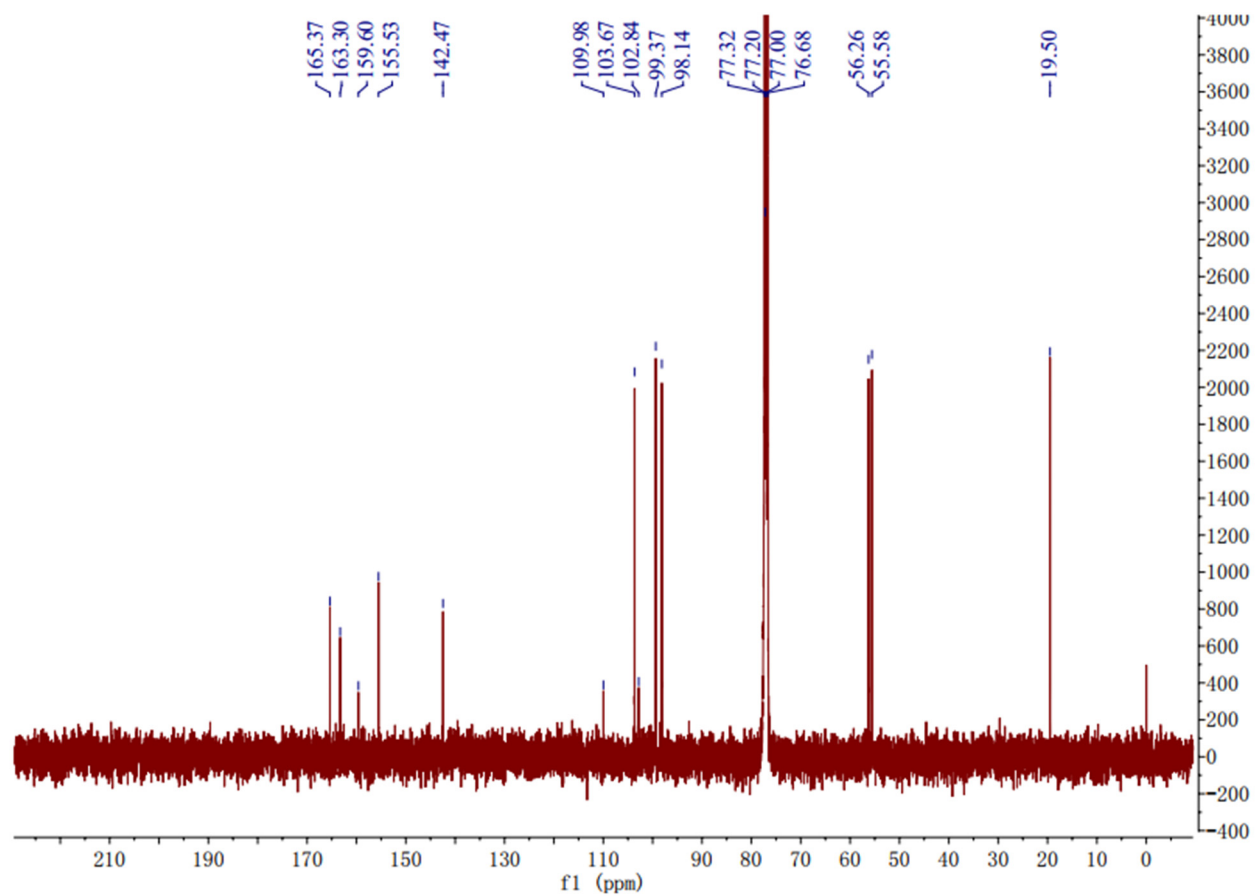


Figure S30. ^{13}C NMR spectrum of 6,8-dimethoxy-3-methylisocoumarin (**8**) in CDCl_3 (100 MHz).

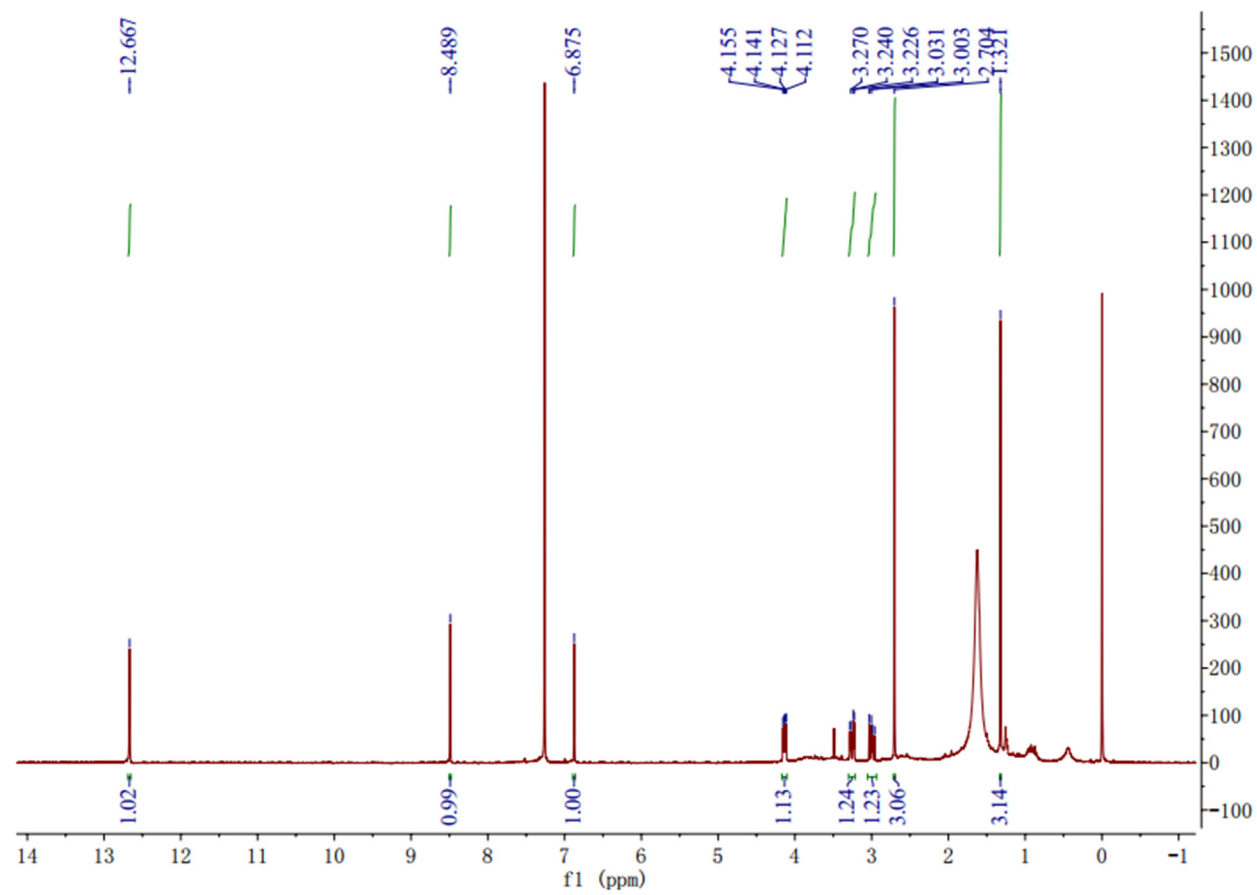


Figure S31. ^1H NMR spectrum of monaspurpurone (**9**) in CDCl_3 (400 MHz).

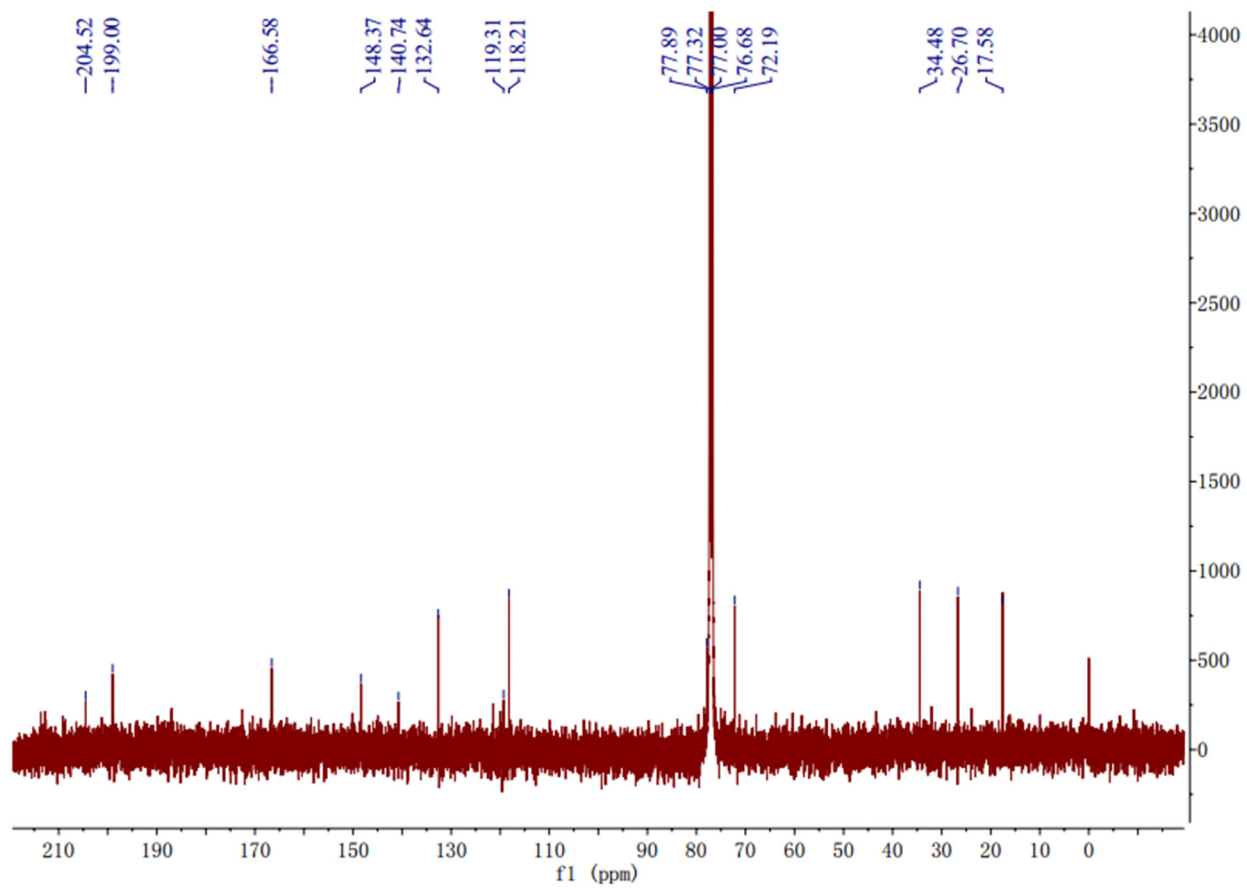


Figure S32. ^{13}C NMR spectrum of monaspurpurone (**9**) in CDCl_3 (100 MHz).

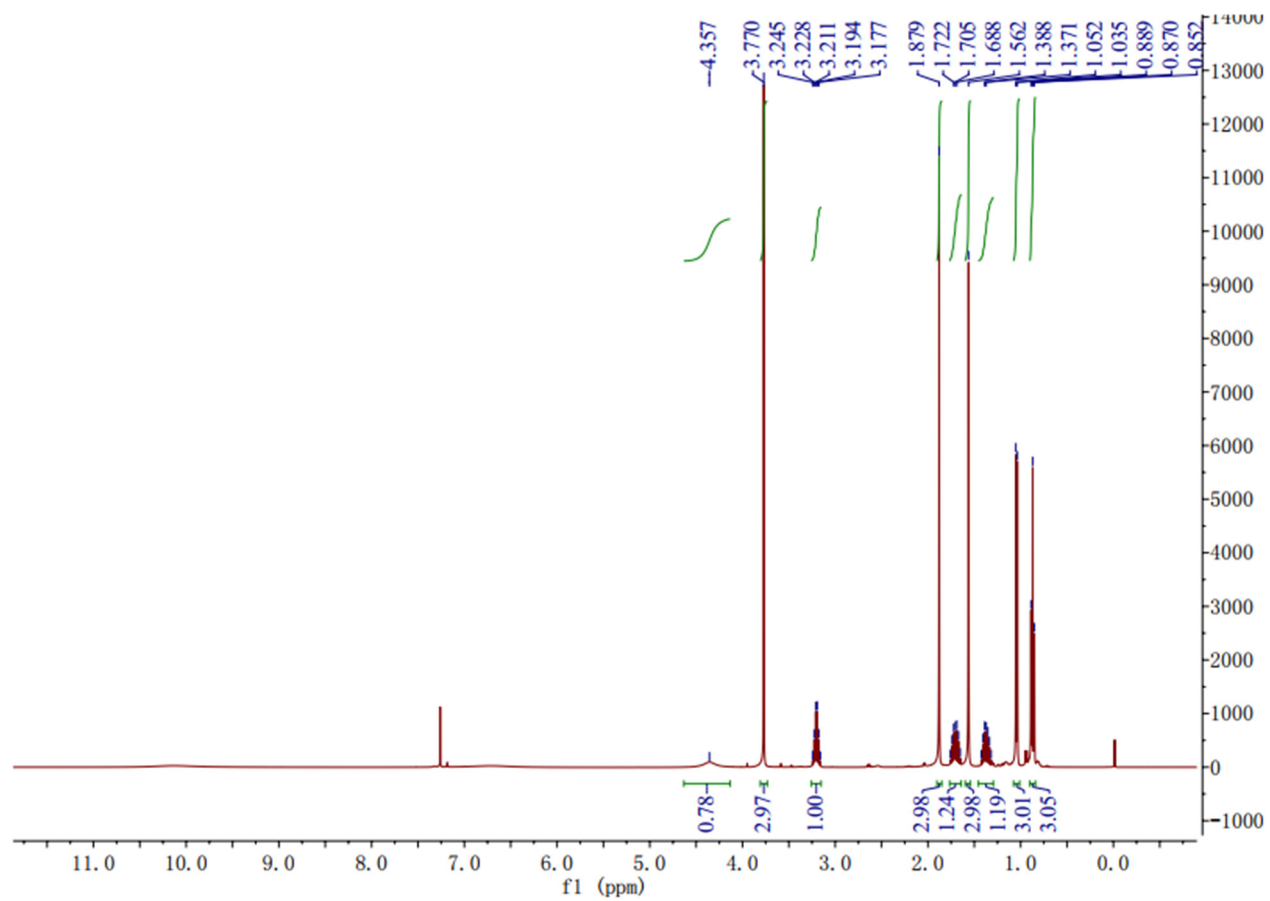


Figure S33. ^1H NMR spectrum of 5-amino-2,6-dimethyl-6-hydroxy-4-(2'-methyl-1-oxobutyl)-3-methoxy-2,4-cyclohexadien-1-one (**10**) in CDCl_3 (400 MHz).

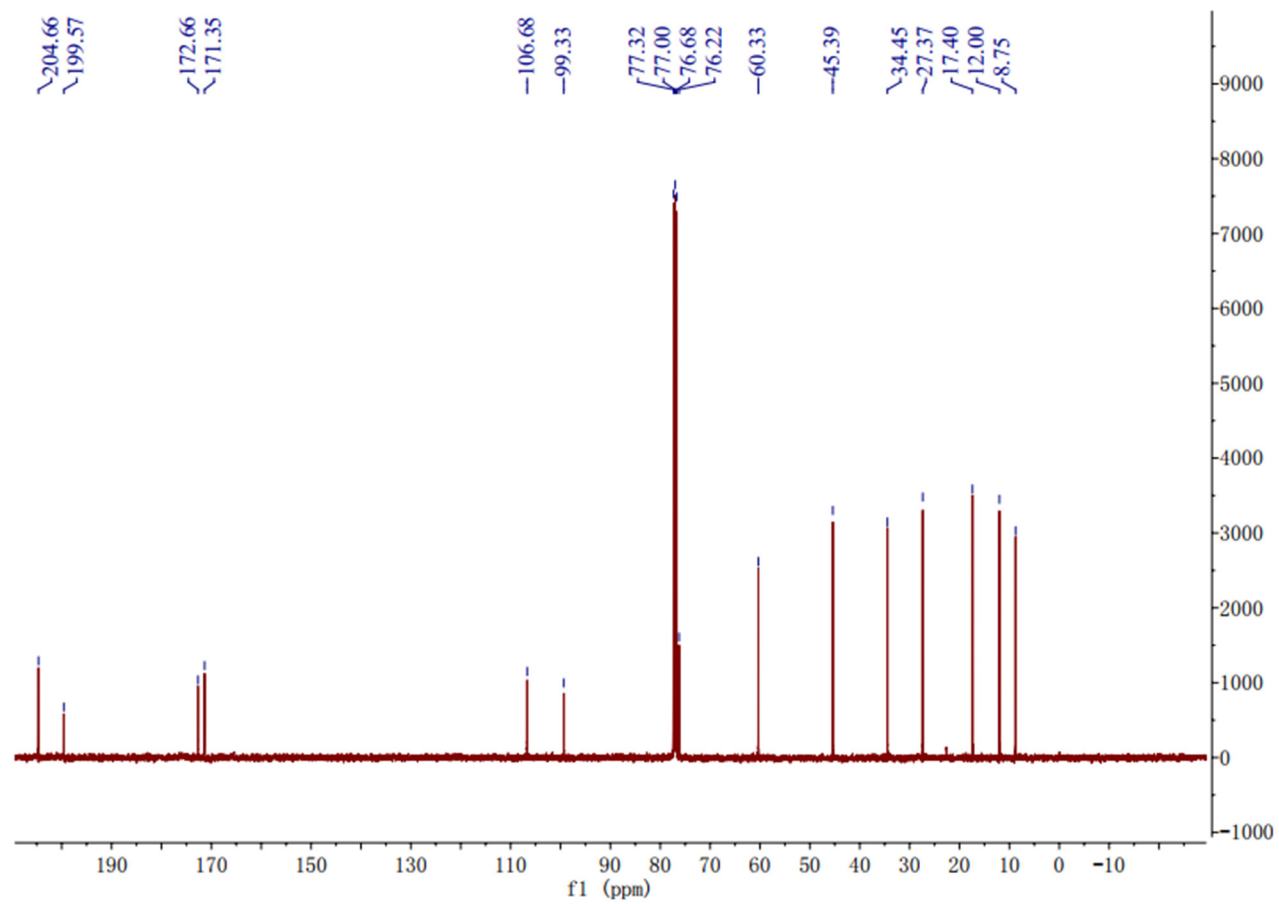


Figure S34. ^{13}C NMR spectrum of 5-amino-2,6-dimethyl-6-hydroxy-4-(2'-methyl-1-oxobutyl)-3-methoxy-2,4-cyclohexadien-1-one (**10**) in CDCl_3 (100 MHz).

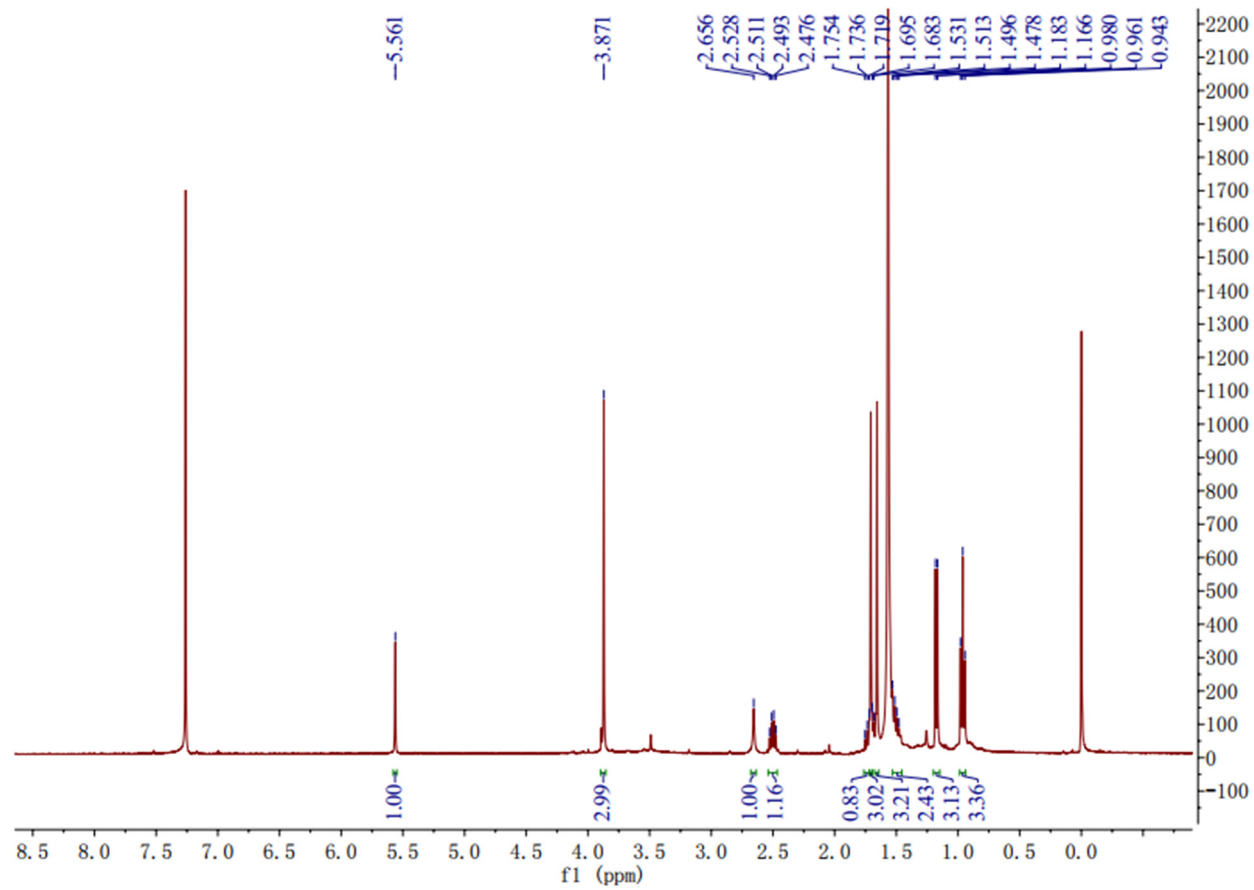


Figure S35. ^1H NMR spectrum of phomaligol A (**11**) in CDCl_3 (400 MHz).

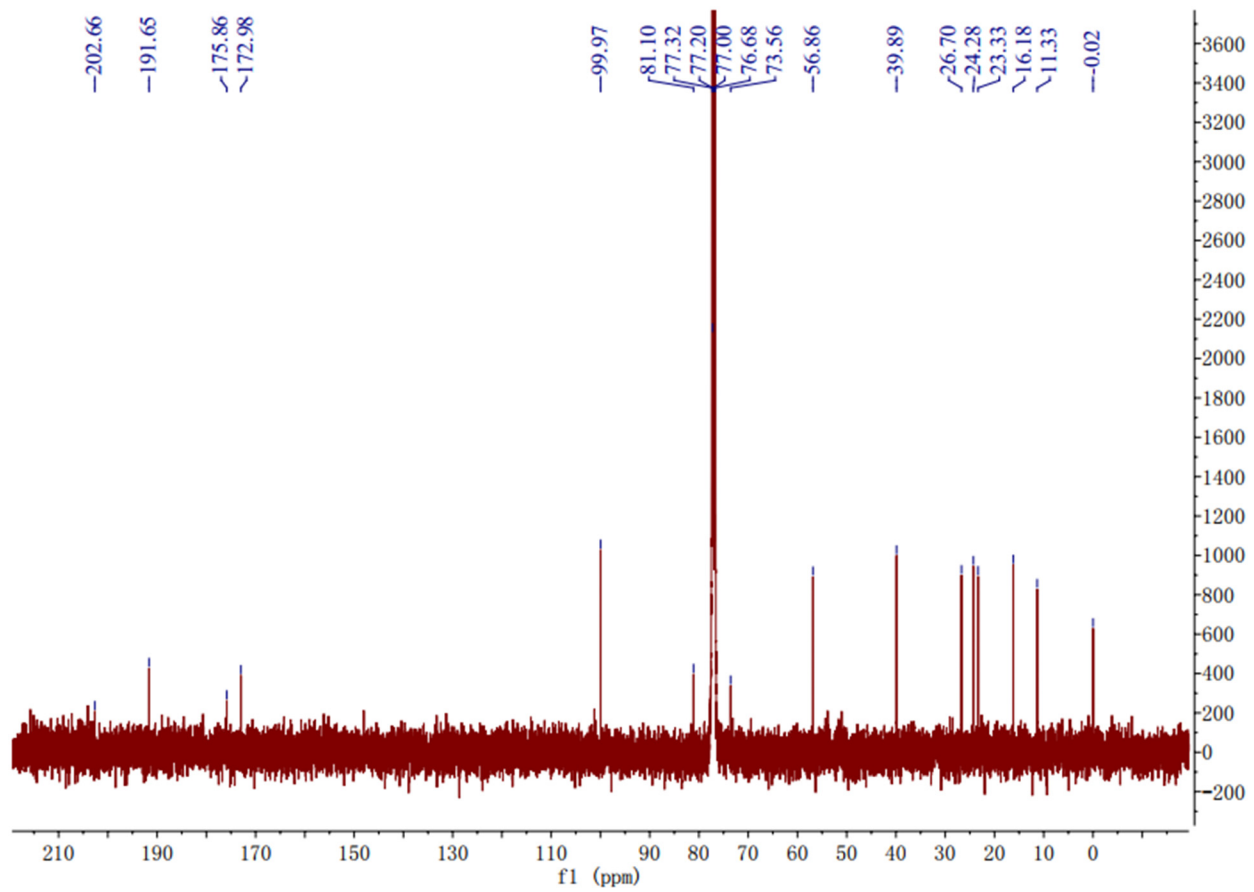


Figure S36. ^{13}C NMR spectrum of phomaligol A (**11**) in CDCl_3 (100 MHz).

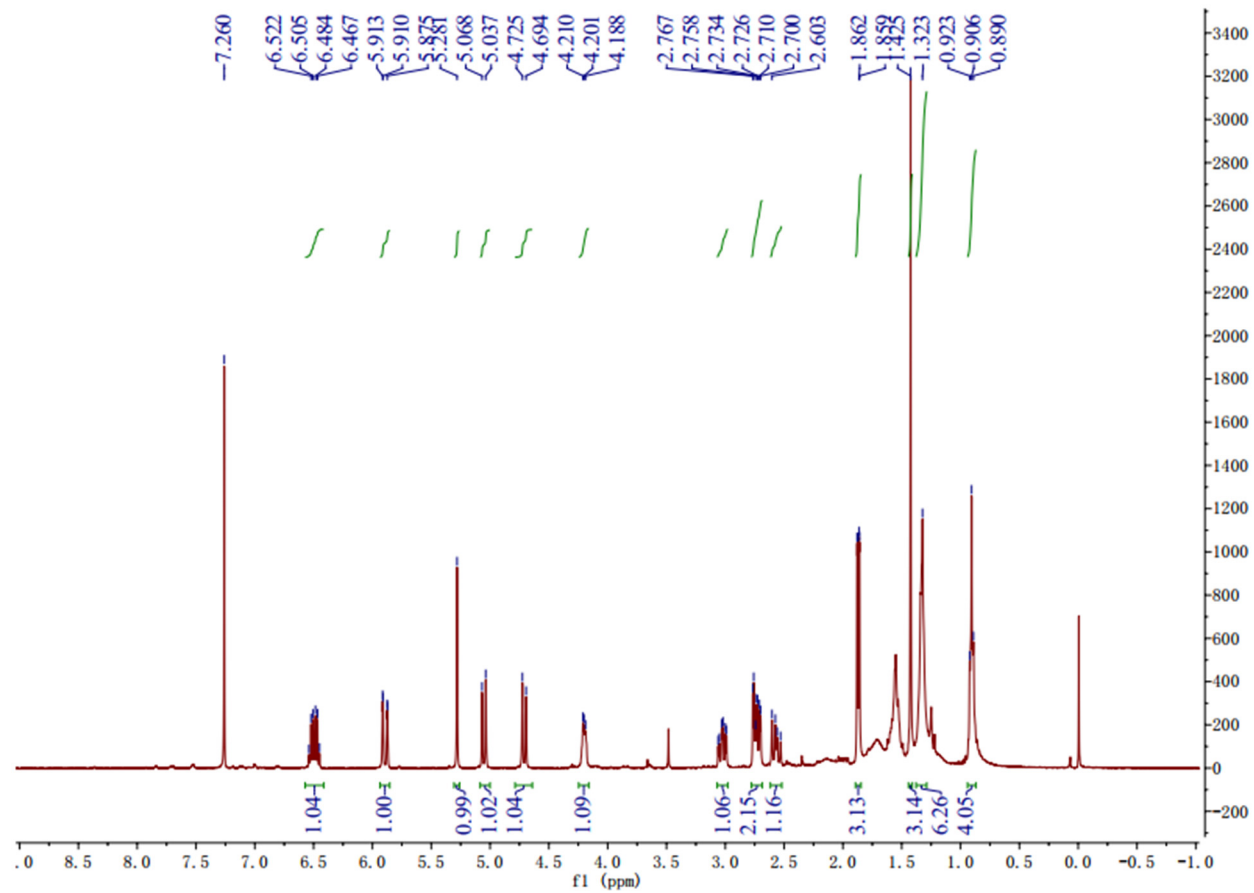


Figure S37. ^1H NMR spectrum of monascuspiloin (**12**) in CDCl_3 (400 MHz).

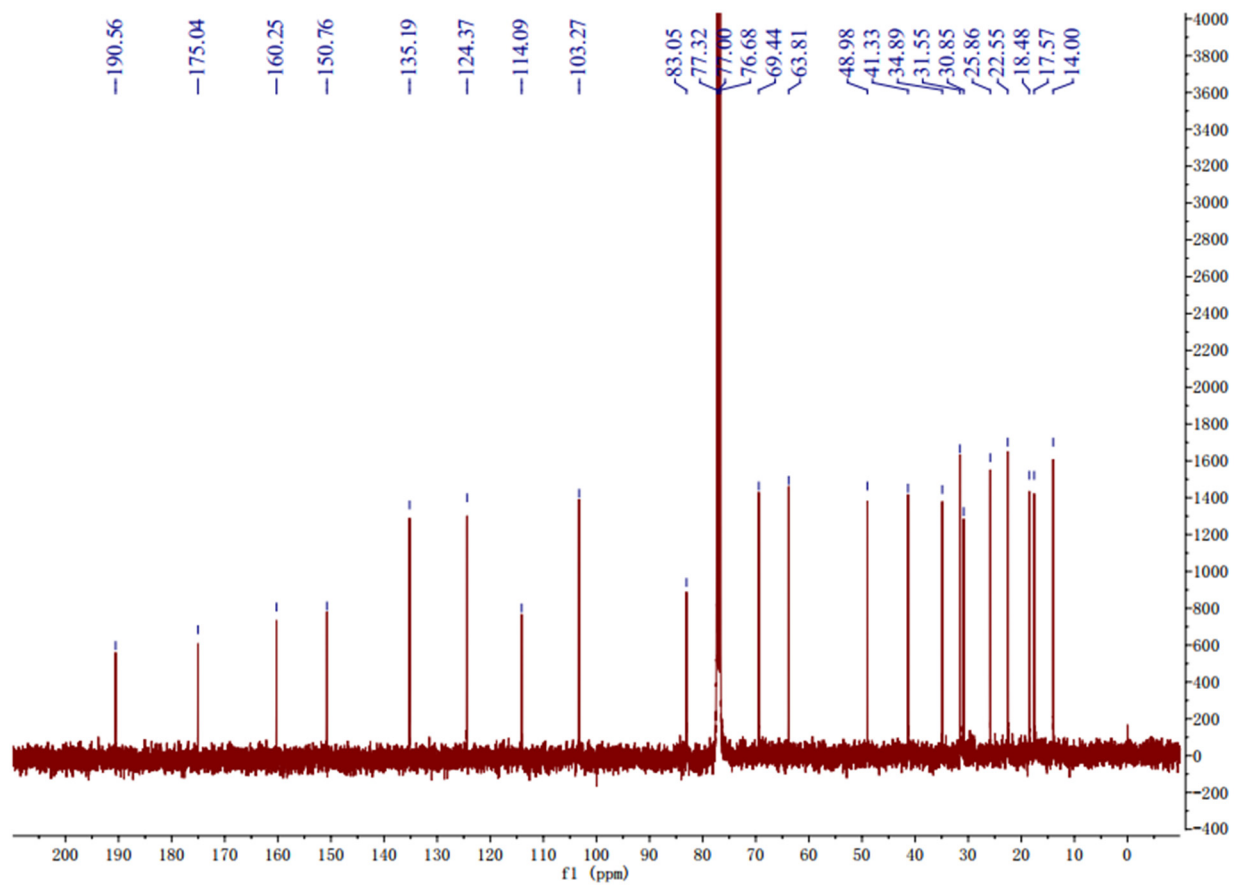
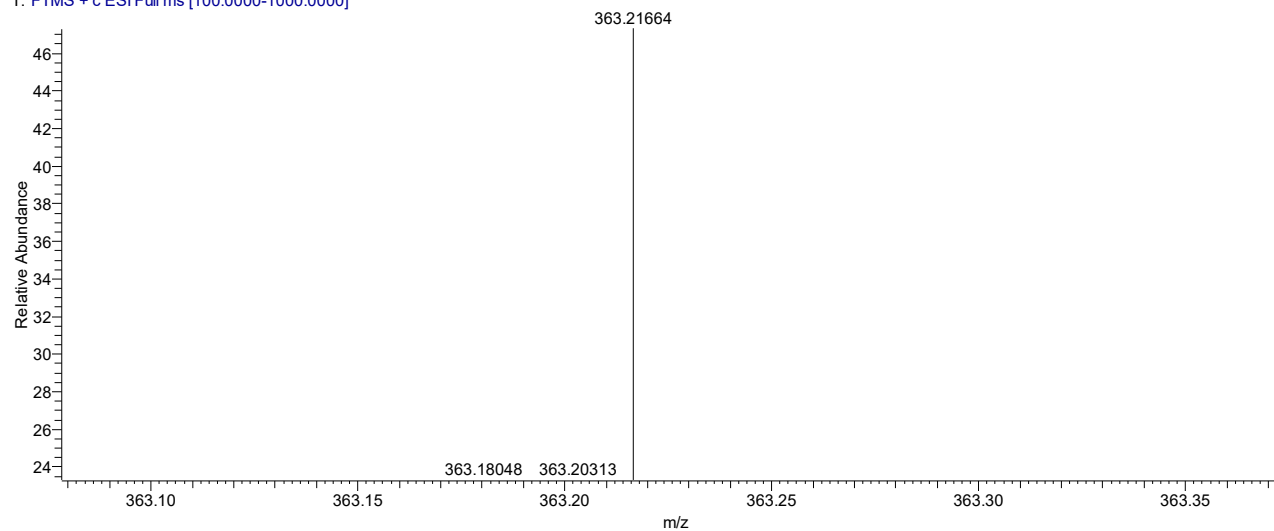


Figure S38. ^{13}C NMR spectrum of monascuspiloin (**12**) in CDCl_3 (100 MHz).

1904A0534-1_ESI#3 RT: 0.03 AV: 1 NL: 2.14E6
T: FTMS + c ESI Full ms [100.0000-1000.0000]



SPECTRUM -simulation :

m/z	Theo. Mass	Delta (ppm)	RDB equiv.	Composition
363.21664	363.21664	0.11	6.5	C ₂₁ H ₃₁ O ₅

Figure S39. HR-(+) ESI-MS spectrum of monarubin C (**13**).

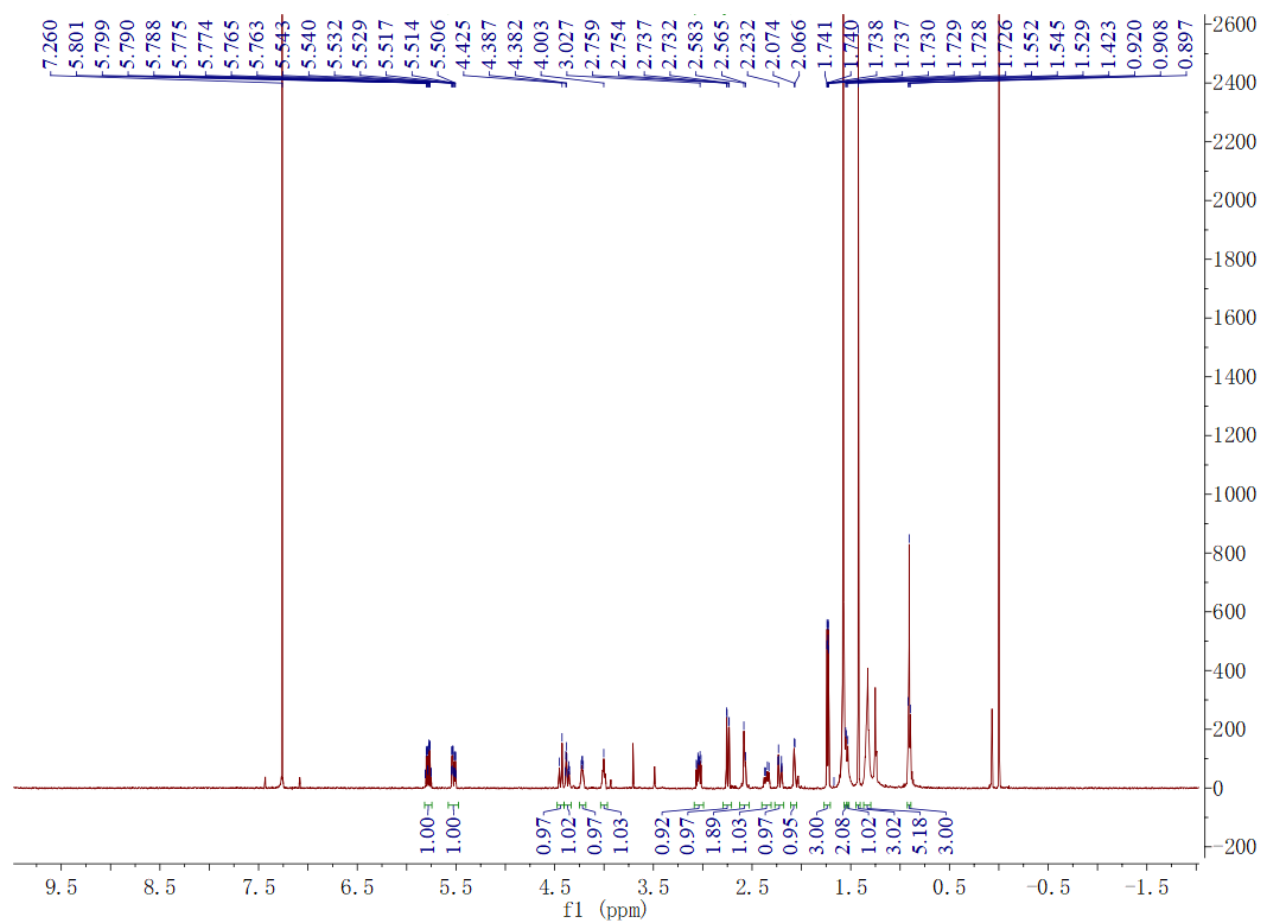


Figure S40. ^1H NMR spectrum of monarubin C (**13**) in CDCl_3 (600 MHz).

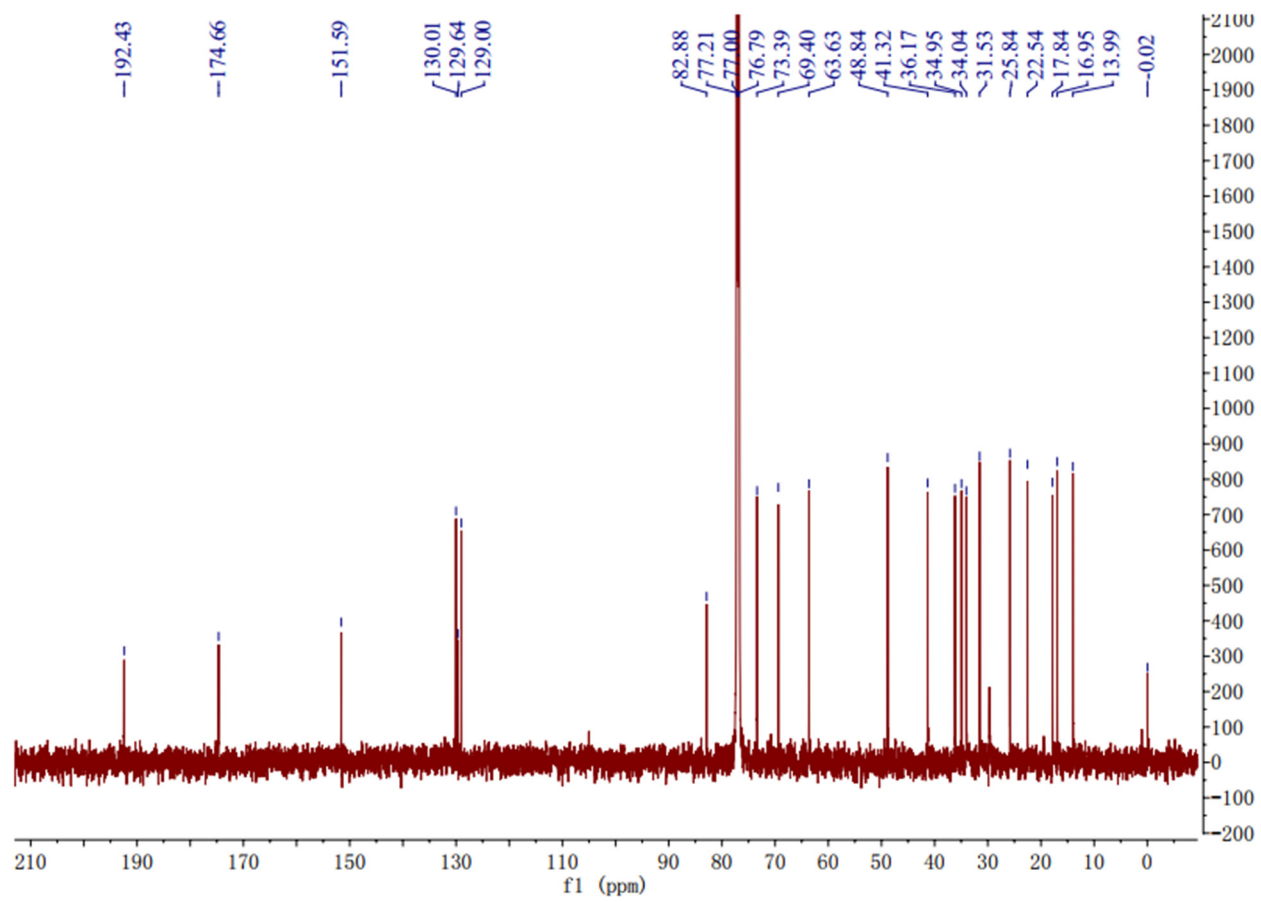


Figure S41. ^{13}C NMR spectrum of monarubin C (**13**) in CDCl_3 (150 MHz).

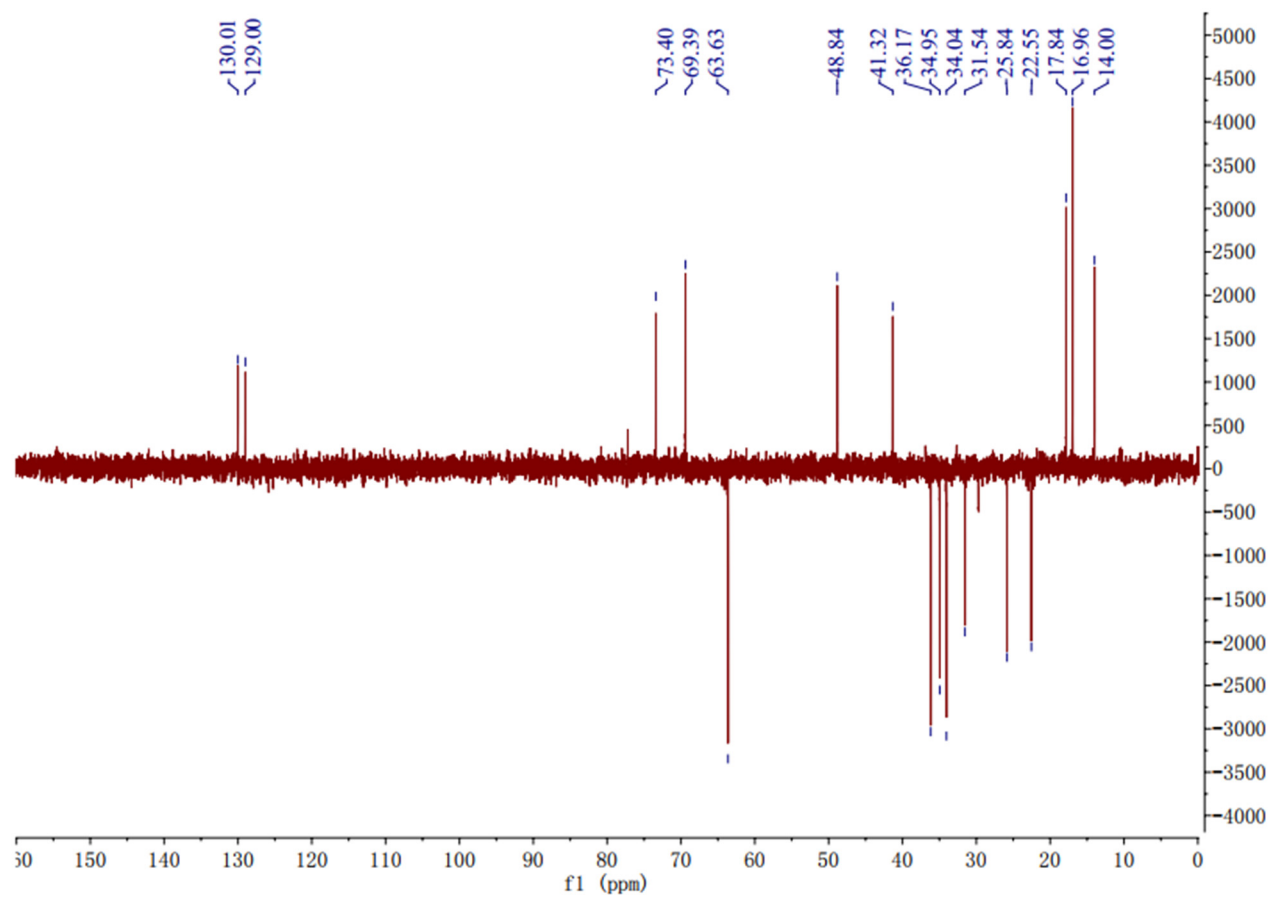


Figure S42. DEPT 135 spectrum of monarubin C (**13**) in CDCl₃ (150 MHz).

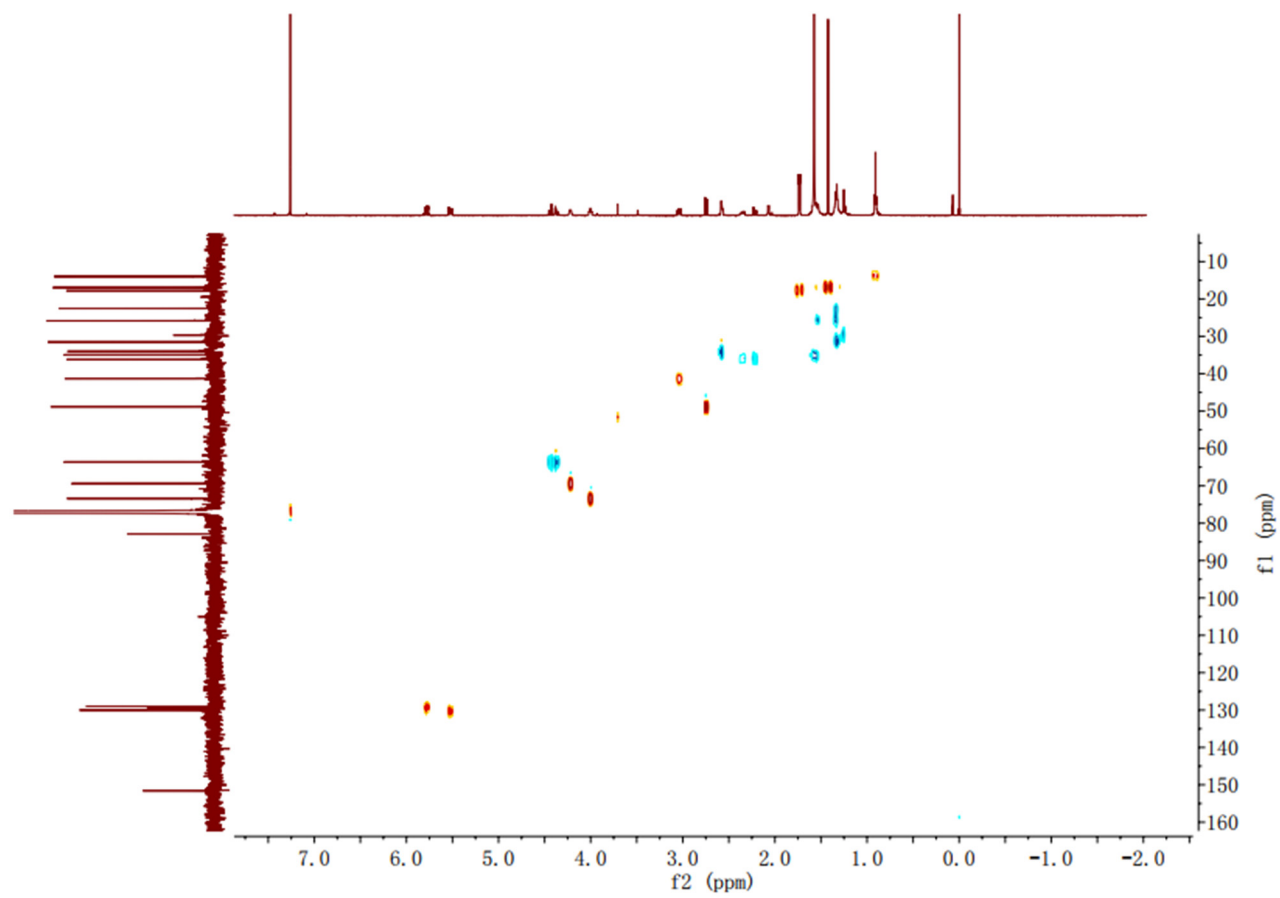


Figure S43. HMQC spectrum of monarubin C (**13**) in CDCl_3 .

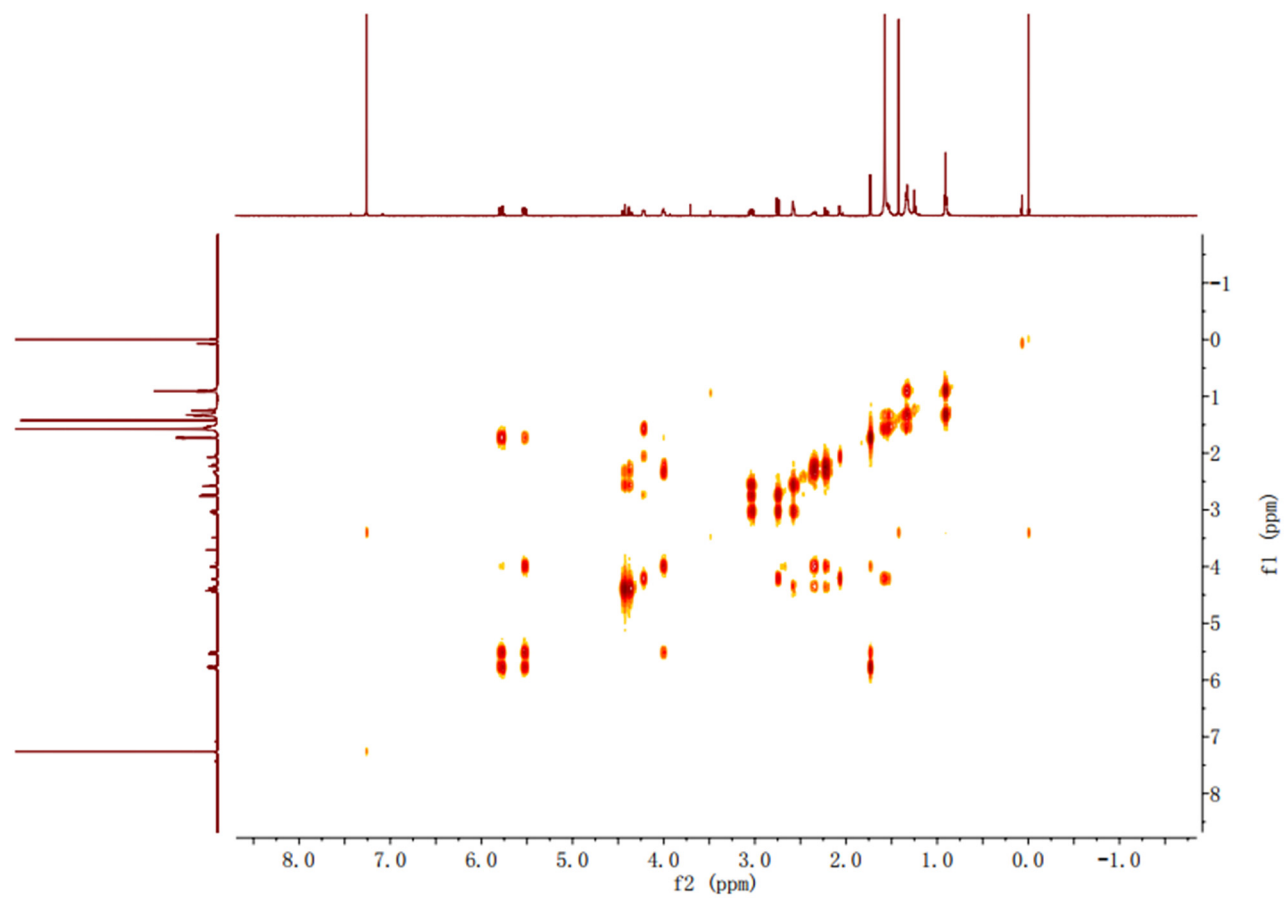


Figure S44. ^1H - ^{13}C HOSY spectrum of monarubin C (**13**) in CDCl_3 .

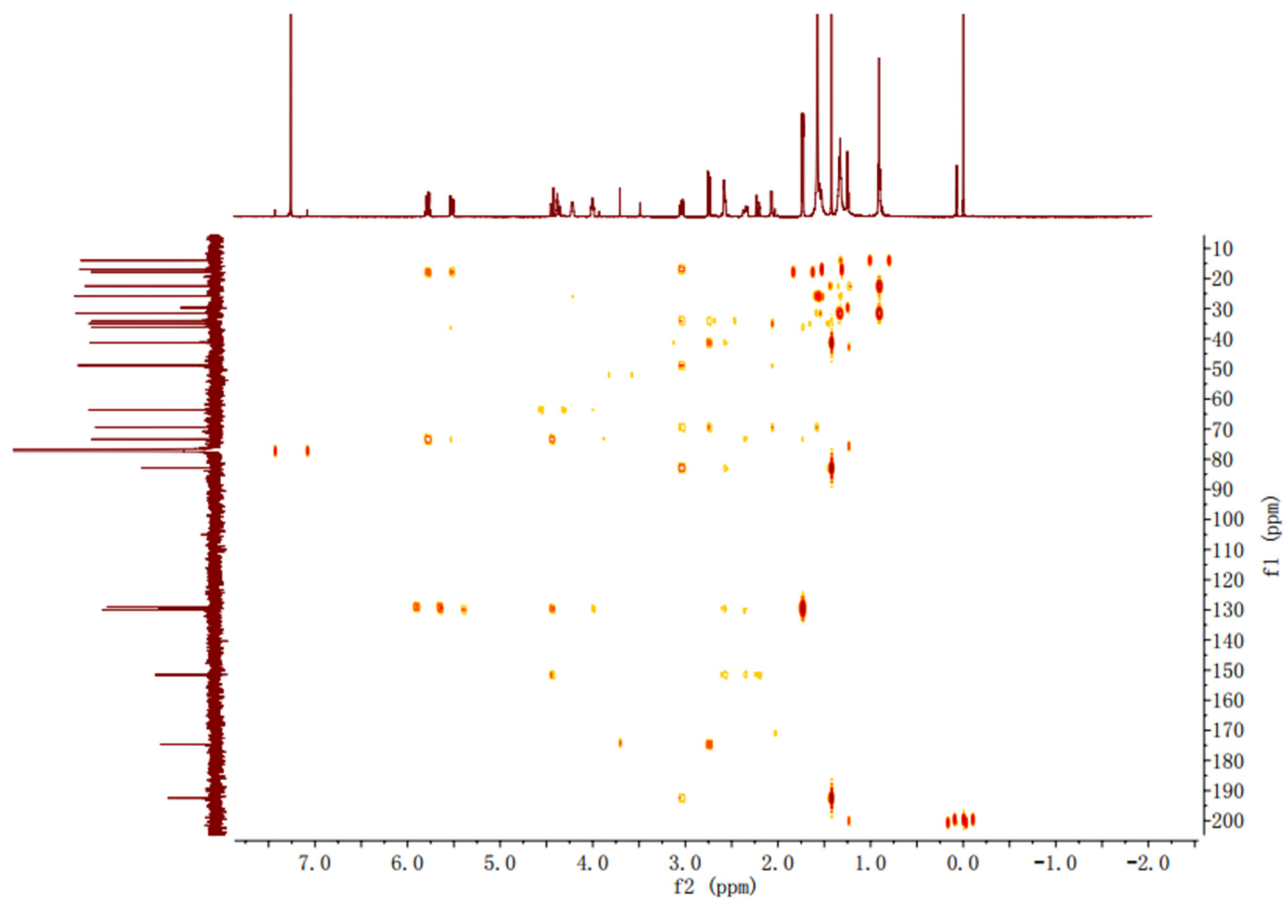


Figure S45. HMBC spectrum of monarubin C (**13**) in CDCl_3 .

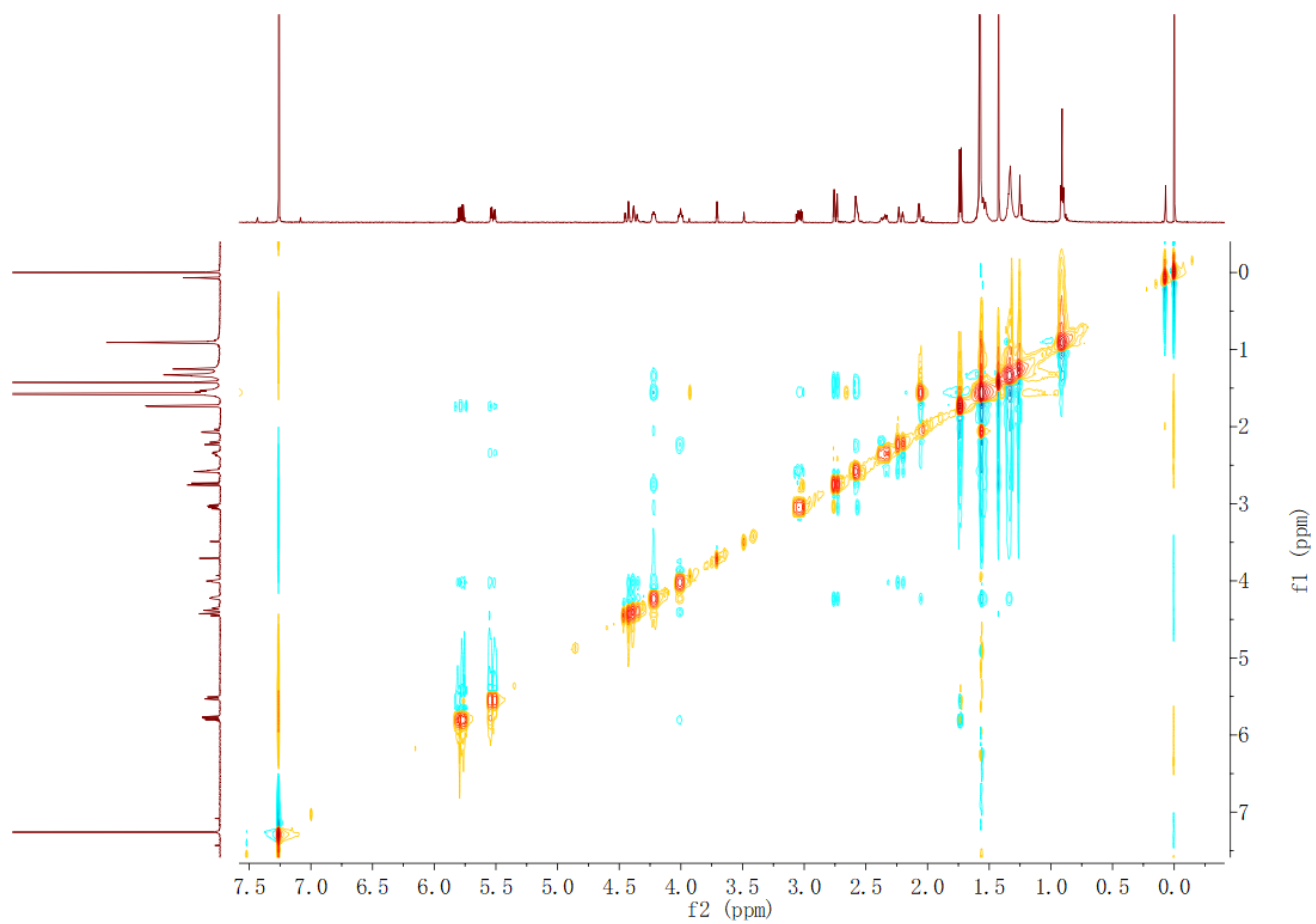


Figure S46. NOESY spectrum of monarubin C (**13**) in CDCl₃.

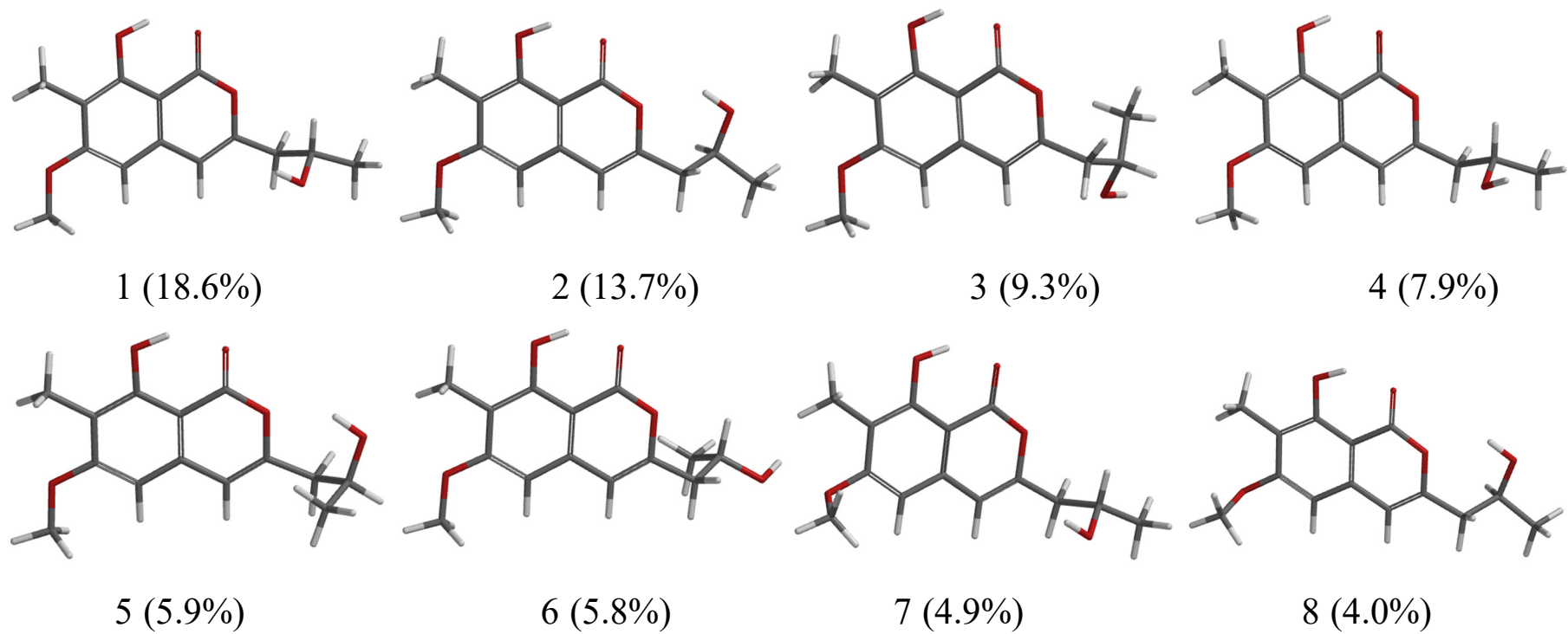


Figure S47. The most stable conformers of 11S-6 calculated at the B3LYP/6-31+G(d) level. Relative populations are in parentheses.

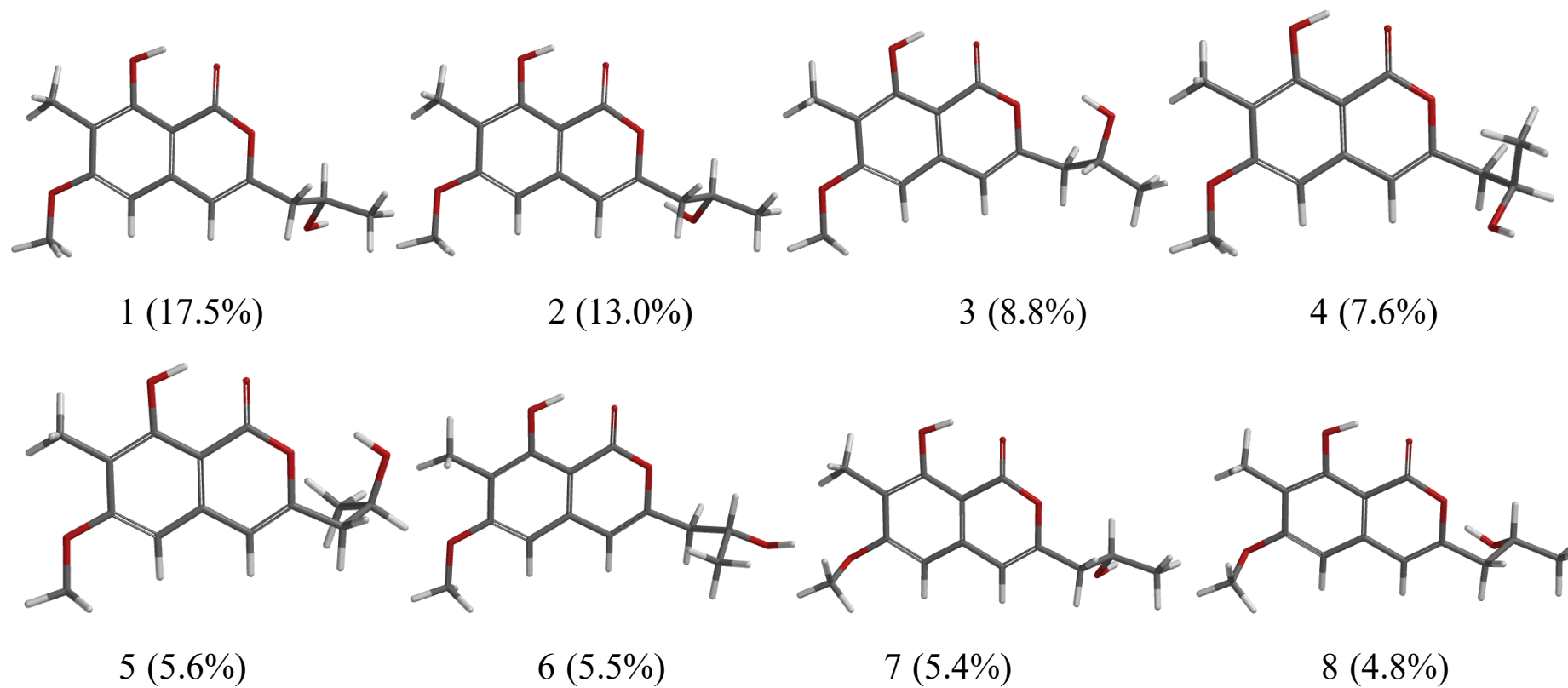


Figure S48. The most stable conformers of 11R-6 calculated at the B3LYP/6-31+G(d) level. Relative populations are in parentheses.

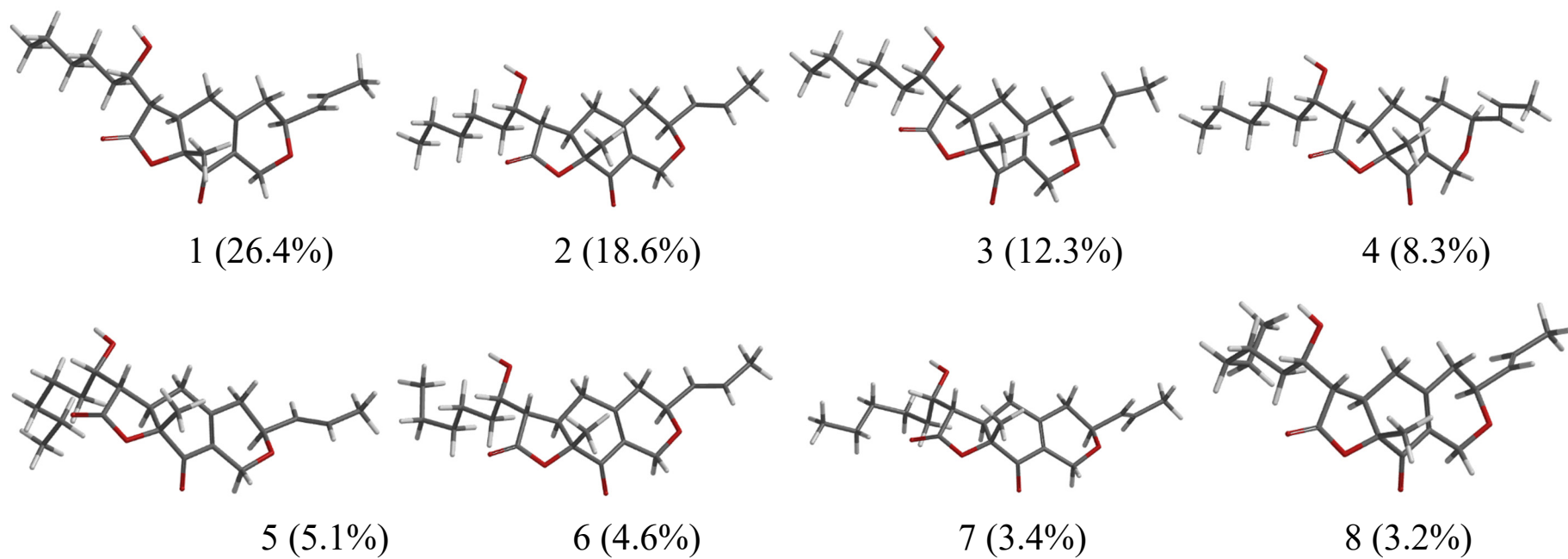


Figure S49. The most stable conformers of 3*S*,6*R*,7*S*,11*S*,17*R*-**13** calculated at the B3LYP/6-31+G(d) level. Relative populations are in parentheses.

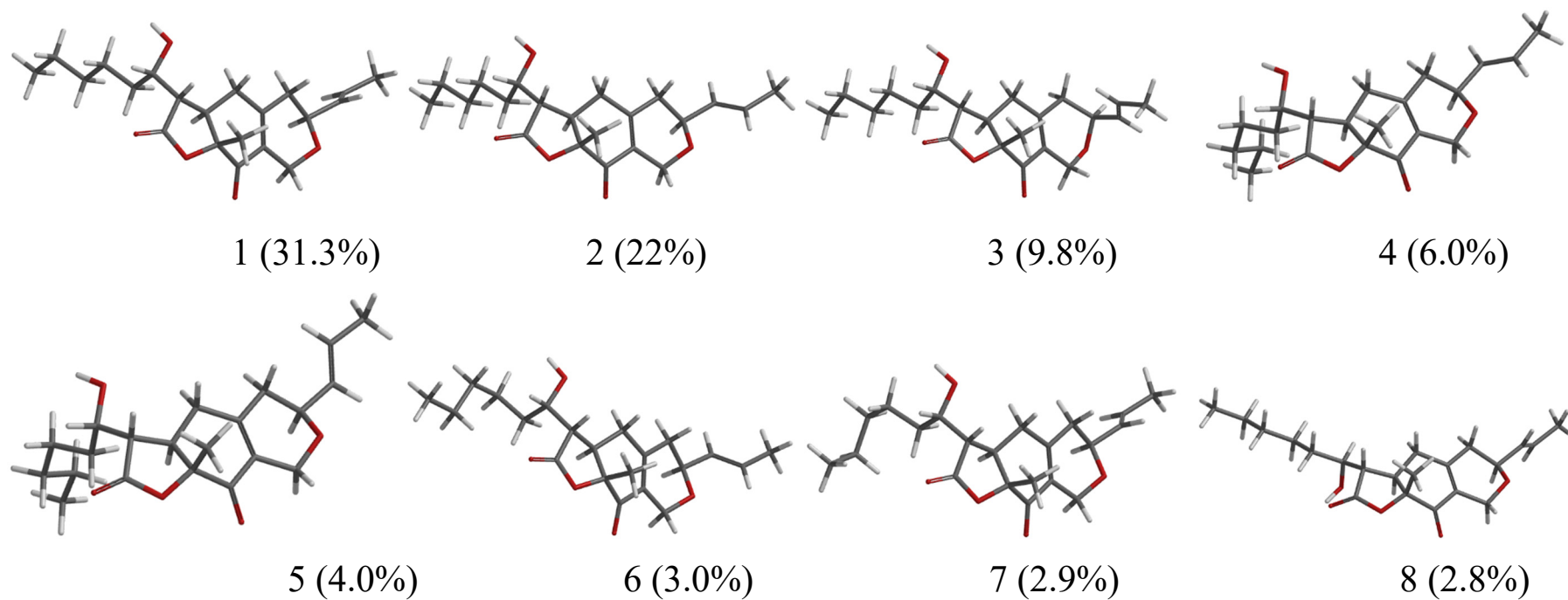


Figure S50. The most stable conformers of *3S,6R,7S,11S,17S-13* calculated at the B3LYP/6-31+G(d) level. Relative populations are in parentheses.

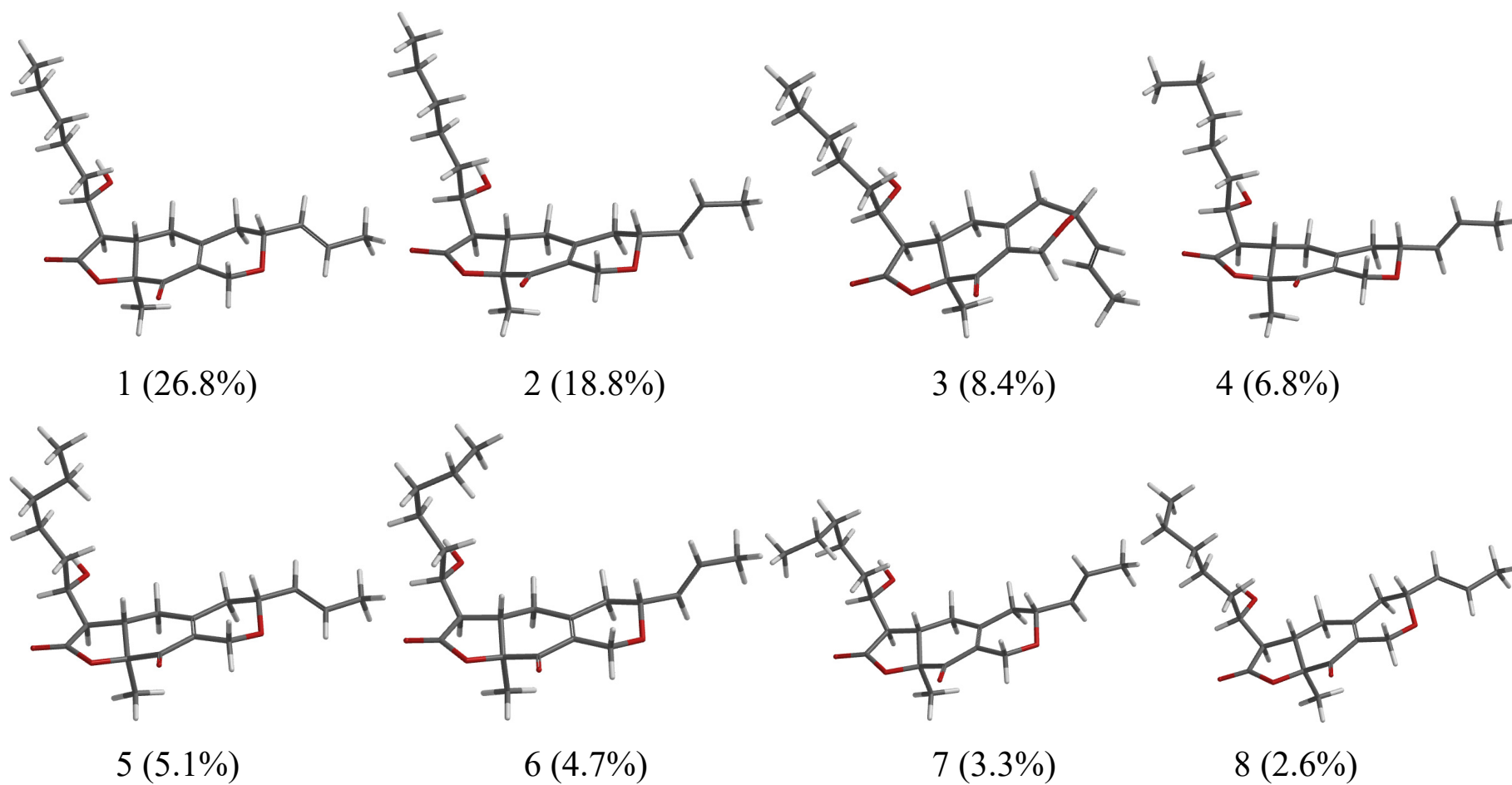


Figure S51. The most stable conformers of *3R,6S,7R,11R,17S-13* calculated at the B3LYP/6-31+G(d) level. Relative populations are in parentheses.

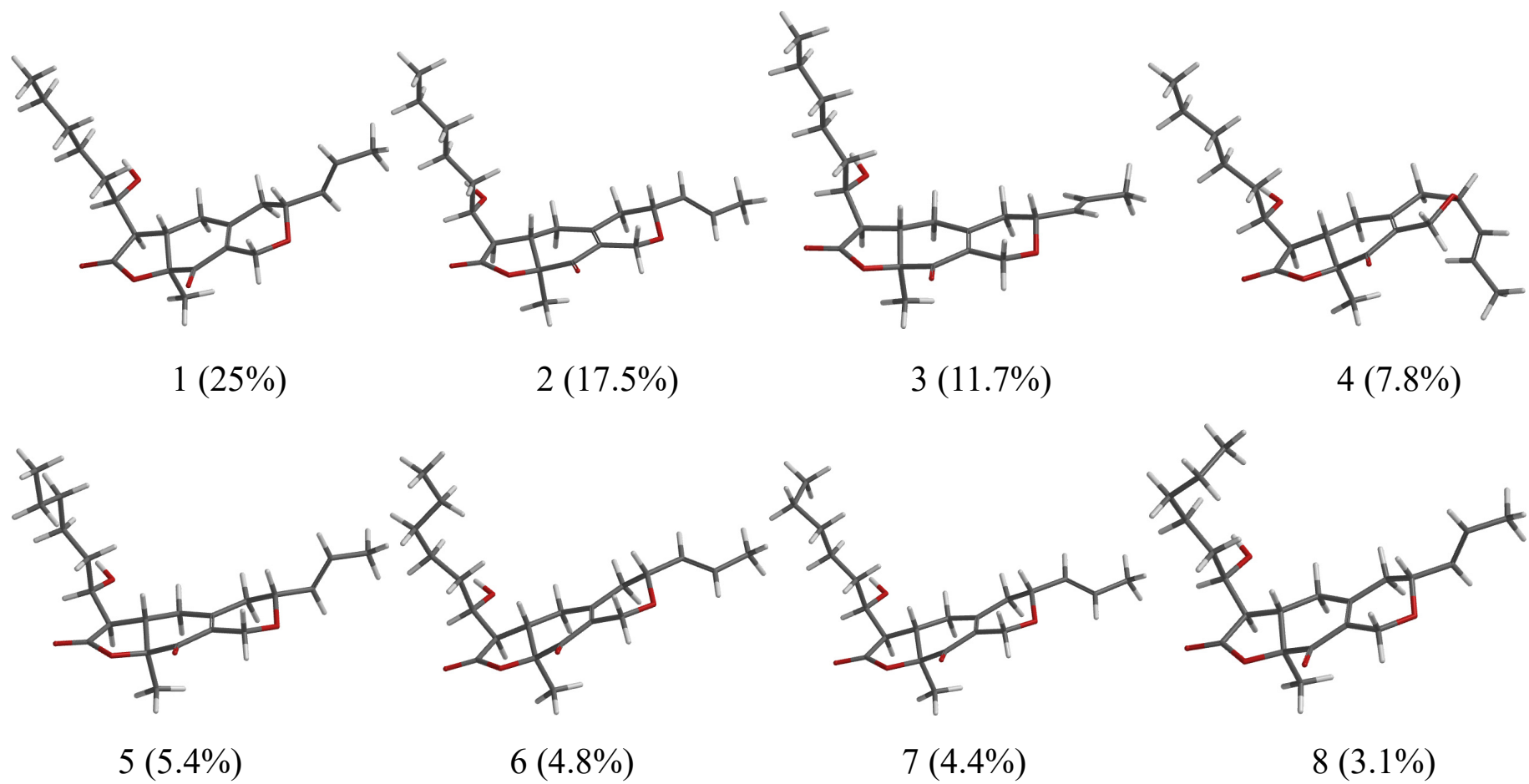


Figure S52. The most stable conformers of *3R,6S,7R,11R,17R-13* calculated at the B3LYP/6-31+G(d) level. Relative populations are in parentheses.

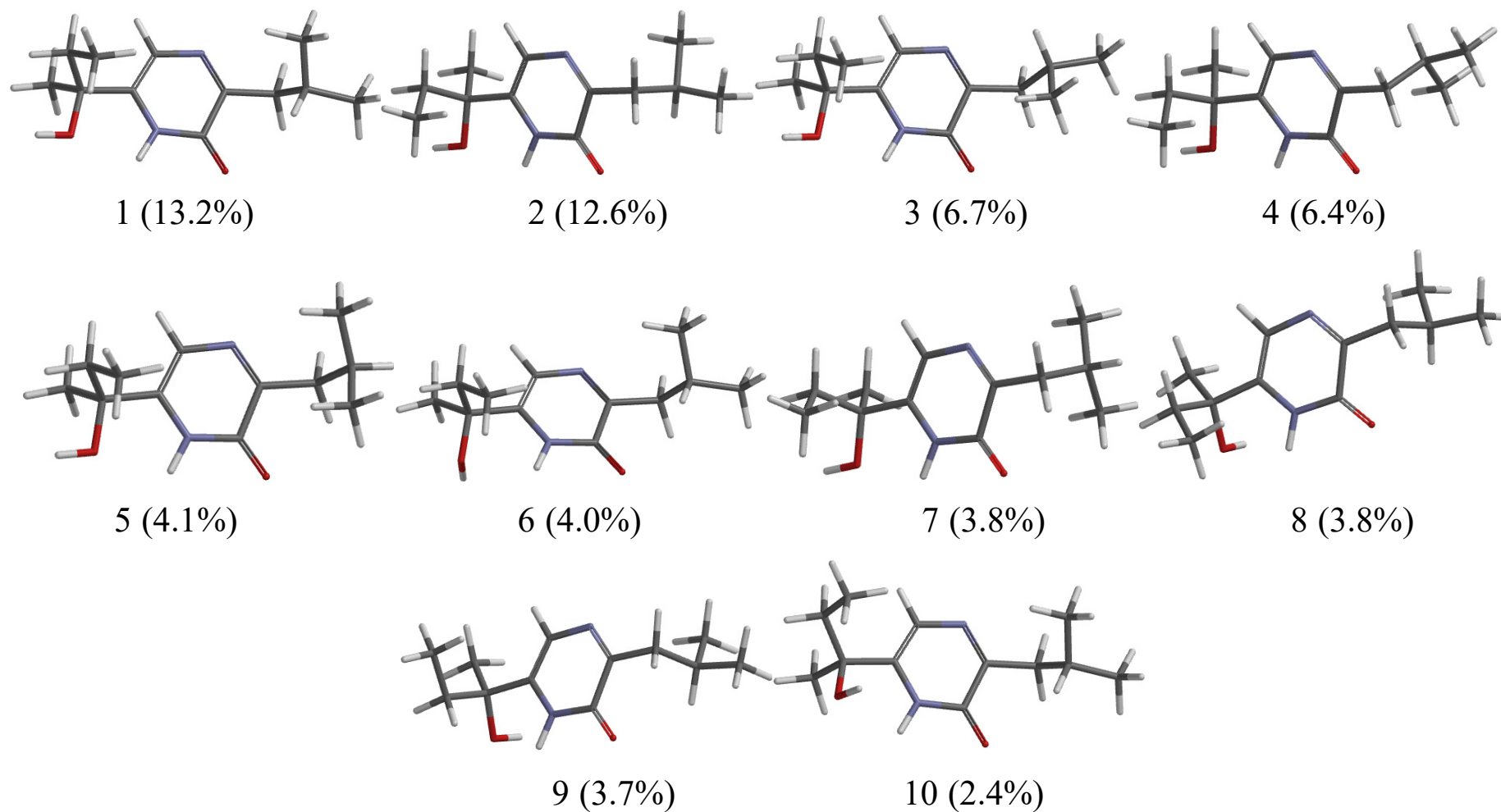


Figure S53. The most stable conformers of 11S-3 calculated at the B3LYP/6-31+G(d) level. Relative populations are in parentheses.

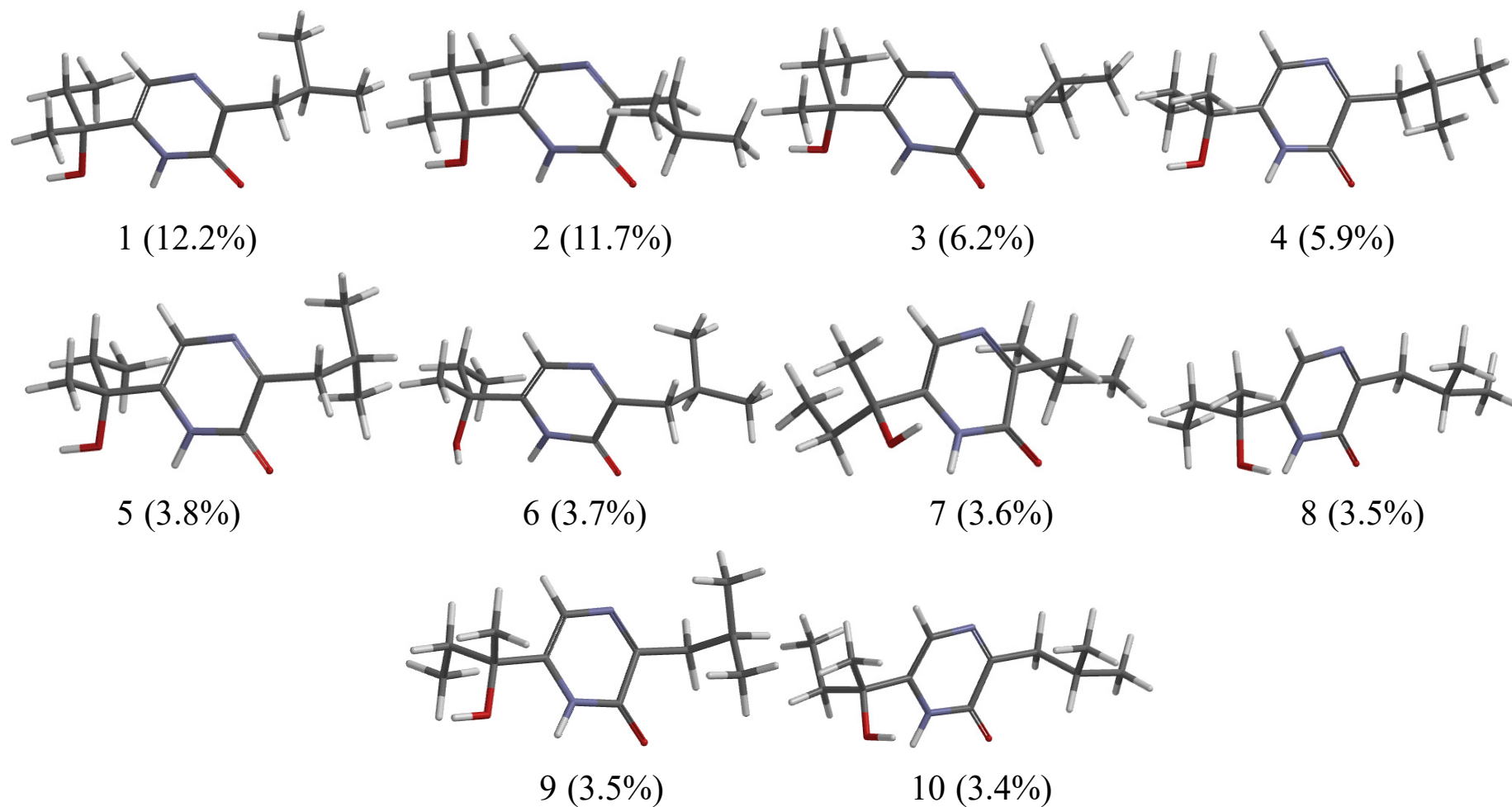


Figure S54. The most stable conformers of 11R-3 calculated at the B3LYP/6-31+G(d) level. Relative populations are in parentheses.

Table S1. X-ray Crystallography Data for **4**.

Empirical formula	2(C ₁₂ H ₂₀ N ₂ O ₂)
Formula weight	448.60
Temperature/K	249.99(10)
Crystal system	monoclinic
Space group	P2 ₁
a/Å	11.77370(10)
b/Å	6.91360(10)
c/Å	16.5776(2)
α /°	90
β /°	91.3700(10)
γ /°	90
Volume/Å ³	1349.01(3)
Z	2
ρ_{calc} /cm ³	1.104
μ /mm ⁻¹	0.607
F(000)	488.0
Crystal size/mm ³	0.2 × 0.15 × 0.08
Radiation	CuK α (λ = 1.54184)
2 Θ range for data collection/°	7.51 to 148.142
Index ranges	-14 ≤ h ≤ 14, -8 ≤ k ≤ 8, -14 ≤ l ≤ 19
Reflections collected	29460
Independent reflections	5242 [R _{int} = 0.0525, R _{sigma} = 0.0221]
Data/restraints/parameters	5242/1/299
Goodness-of-fit on F ²	1.039

Final R indexes [$I \geq 2\sigma(I)$]	$R_1 = 0.0570$, $wR_2 = 0.1619$
Final R indexes [all data]	$R_1 = 0.0588$, $wR_2 = 0.1647$
Largest diff. peak/hole / $e \text{ \AA}^{-3}$	0.52/-0.22
Flack parameter	-0.04(7)

Table S2. The hepatocellular carcinoma cell line HepG2 activity of manorubin B (6)

HepG2								
	DMSO (μL)	manorubin B (6) (μmol/L)						
	0.054	0.037	0.111	0.333	1	3	9	27
OD (570nm) ^a	1.44	1.437	1.377	1.294	0.996	0.454	0.388	0.379
Cell viability (100%) ^b		96.3	94.7	91.2	66.3	32.4	24.5	27.7
Inhibition rate (100%) ^c		3.7	5.3	8.8	33.7	67.6	75.5	72.3

^a Average of three measurements, OD: Optical density, ^b Cell viability = Measurements value (OD)/Control value DMSO (OD) × 100%,

^c Inhibition rate = 100% – Cell viability.

Table S3. The hepatocellular carcinoma cell line QGY7701 activity of manorubin B (6)

QGY7701								
	DMSO (μL)	manorubin B (6) (μmol/L)						
	0.054	0.037	0.111	0.333	1	3	9	27
OD (570nm)	1.46	1.320	1.310	1.147	0.423	0.255	0.235	0.188
Cell viability (100%)		90.2	89.5	78.4	28.9	17.4	16.1	12.8
Inhibition rate (100%)		9.8	10.5	21.6	71.1	82.6	83.9	87.2

Table S4. The nasopharyngeal carcinoma cell line SUNE1 activity of lunatinin (7)

SUNE1								
	DMSO (μ L)	lunatinin (7) (μ mol/L)						
	0.2	1.5625	3.125	6.25	12.5	25	50	100
OD (570nm)	0.791	0.668	0.672	0.578	0.452	0.391	0.364	0.368
Cell viability (100%)		84.5	84.9	73	57.2	49.5	46.1	46.5
Inhibition rate (100%)		15.5	15.1	27	42.8	50.5	53.9	53.5

Table S5. The hepatocellular carcinoma cell line HepG2 activity of lunatinin (7)

HepG2								
	DMSO (μ L)	lunatinin (7) (μ mol/L)						
	0.2	1.5625	3.125	6.25	12.5	25	50	100
OD (570nm)	0.422	0.373	0.347	0.233	0.142	0.111	0.085	0.092
Cell viability (100%)		88.3	82.3	55.3	33.6	26.2	20.1	21.7
Inhibition rate (100%)		11.7	17.7	44.7	66.4	73.8	79.9	78.3

Table S6. The hepatocellular carcinoma cell line QGY7701 activity of lunatinin (7)

QGY7701								
	DMSO (μ L)	lunatinin (7) (μ mol/L)						
	0.2	1.5625	3.125	6.25	12.5	25	50	100
OD (570nm)	0.976	0.915	0.758	0.479	0.216	0.162	0.102	0.097
Cell viability (100%)		93.8	77.7	49.1	22.1	16.6	10.4	9.9
Inhibition rate (100%)		6.2	22.3	5.9	77.9	83.4	89.6	90.0